Shahrood University of Technology

Journal of Mining and Environment (JME)

Journal homepage: www.jme.shahroodut.ac.ir

Iranian Society of Mining Engineering (IRSME)

Preparation of Iron Ore Specimens Containing Non-Persistent Edge Notches for Dynamic Testing: Geometry and Configuration of Notches

Shadman Mohammadi Bolbanabad[1], Vahab Sarfarazi[2*], and Masoud Monjezi[1]

1. Department of Mining Engineering, Faculty of Mining and Materials, Tarbiat Modares University, Tehran, Iran
2. Department of Mining Engineering, Hamedan University of Technology, Hamedan, Iran

Article Info

Received 4 September 2025
Received in Revised form 21 November 2025
Accepted 29 November 2025
Published online 29 November 2025

DOI: 10.22044/jme.2025.16775.3292

Keywords

SHPB
Non-persistent edge notch
Dynamic testing
Specimen preparation methodology

Abstract

One of the critical steps in experimental research is the precise preparation of specimens. This study aims to develop and present a comprehensive methodology for preparing magnetite iron ore specimens containing non-persistent edge notches for dynamic testing, as well as iron ore and ice specimens for uniaxial and Brazilian tests. Core drilling was performed using diamond drills with diameters of 54 mm for uniaxial and Brazilian tests and 22 mm for dynamic Split Hopkinson Pressure Bar (SHPB) tests. Non-persistent edge notches with a thickness of 3 mm, controlled length, and inclination were created using a cutter, and their geometric quality was verified through meticulous inspection. For ice specimens, filling the notches with water in tubes matching the specimen diameter provided optimal uniformity and stability. Additionally, precise control of parameters such as core and drill parallelism, drilling speed, cooling water flow, and environmental conditions (dry, saturated, and frozen) preserved the structural integrity and quality of the specimens. The results demonstrated that systematically following these procedures, along with detailed documentation of geometric and environmental specimen features, enables the production of intact, standardized, and reproducible specimens, ensuring reliable and consistent examination of the mechanical response and fracture of magnetite iron ore under both dynamic and quasi-static conditions.

1. Introduction

The mechanical and behavioral characteristics of natural rocks are governed by multiple geological and structural factors. These include uniaxial compressive and tensile strength, deformability, hardness and abrasiveness, the occurrence of quartz veins and other abrasive minerals, faults and shear zones, the degree of fragmentation, as well as the type, dip, and orientation of joints [1–3]. These characteristics reflect the inherent heterogeneity and anisotropy of rocks and can directly affect the outcomes of mechanical tests (Figure 1). Therefore, to accurately explore the response of natural rocks at various loading conditions in the laboratory, proper specimen preparation that preserves the structural integrity and natural conditions of the rock is essential. This preparation process involves selecting homogeneous blocks from the quarry, avoiding large joints, weathered zones, and non-uniform mineral veins, followed by coring, geometric cutting, and polishing of the specimens.

Over the past decade, numerous efforts have been reported for the preparation of physical specimens for uniaxial compression tests. These studies have not only investigated various specimen preparation methods but also evaluated the effects of specimen geometry and the presence of discontinuities on mechanical behavior. A brief overview of some notable research in this field is presented below:

Sarfarazi et al. [4] used gypsum specimens to investigate the fracture characteristics of F-shaped, non-persistent notches under uniaxial loading. To create these artificial cracks, 1-mm-thick aluminum plates were inserted into 50-mm-thick plastic foam. Fu et al. [5] employed cylindrical

Corresponding author: Sarfarazi@hut.ac.ir (V. Sarfarazi)

molds to prepare disk specimens containing a central notch. The notch was produced by placing an aluminum plate at the center of the cylinder inside the plastic foam. For semicircular specimens with edge notches, the cylinder was divided into two halves, and an aluminum plate was positioned within the foam to form the notch. Bagher Shemirani et al. [6] studied the interaction between a concrete-gypsum interface containing a central notch. Semicircular concrete and gypsum specimens were prepared and bonded using a stone adhesive to create a synthetic discontinuity (crack) at the interface, which remained unfilled.



Figure 1. Heterogeneous rock mass containing irregular joints.

To examine the mechanical response of specimens with vertical non-persistent notches under uniaxial compression, Fu et al. [7] prepared cubic specimens (100 × 100 × 100 mm) containing vertical notches. Grooves were made at the top and bottom of the molds, and aluminum plates were inserted into these grooves to form the notches. Shakeri et al. [8] used plexiglass cylindrical molds with grooved ends to prepare disk specimens containing multiple non-persistent notches, where aluminum blades were inserted into the grooves to generate the notches. Sarfarazi et al. [9] carried out uniaxial compression tests on gypsum samples (150 × 150 × 60 mm) to investigate the effects of T-shaped non-persistent notch angles and numbers. Notches were formed by placing 1 mm thick steel plates within 50 mm thick plastic foam.

To examine the shear behavior of heterogeneous samples consisting of a gypsum and concrete layer with non-persistent notches, Fu et al. [10] first divided a mold with dimensions of 200 × 200 × 100 mm into two sections using a sheet. Two aluminum blades were then inserted into a plastic foam to create two non-persistent notches. The edge-notched gypsum and concrete specimens were subsequently fabricated and bonded together using adhesive. Fu et al. [11] studied the interaction between the concrete–gypsum interface and edge notches using three-point bending tests. Initially, quarter-circle specimens of gypsum and concrete were prepared, and then the specimens were bonded together using stone adhesive in a manner that produced an edge notch of the desired depth. Haeri et al. [12] prepared gypsum specimens with dimensions of 150 × 150 × 50 mm for investigation of the behavior of non-persistent joints under punch shear loading. The specimen geometry and the configuration of the non-persistent joints were defined by inserting wooden strips and aluminum plates into a foam mold. Haeri et al. [13] fabricated mortar specimens measuring 100 × 100 × 50 mm to examine the response of three non-persistent notches under uniaxial loading. Aluminum plates were inserted into a foam mold to form the non-persistent notches. Asadizadeh et al. [14] implemented uniaxial compression tests on quasi-rock cylindrical specimens with a central discontinuity formed using a plexiglass blade in a

plastic cylinder groove. Sarfarazi et al. [15] employed cylindrical gypsum specimens, 100 mm in diameter and 40 mm thick, to examine the fracture behavior of Y-shaped joints under indirect tensile loading. Non-persistent joints were produced by embedding 1-mm-thick steel plates within a 50-mm-thick foam mold. Zhou et al. [16] prepared semi-circular specimens with edge cracks to evaluate the fracture toughness of concrete by the use of a novel testing method. To introduce the non-persistent notches, 1 mm-thick steel plates were embedded into a 50 mm-thick foam mold.

Sarfarazi et al. [17] fabricated rock-like columnar specimens measuring 150 × 150 × 50 mm to investigate the mechanical response of cavities, half-cavities, and non-persistent joints under uniaxial compression. The non-persistent joints, cavities, and half-cavities were introduced by embedding aluminum plates, cylinders, and semi-cylinders into a 50 mm-thick foam mold. Yang et al. [18] fabricated rock blocks measuring 160 × 80 mm to examine the mechanical behavior of sandstone specimens containing three non-persistent notches under uniaxial compression. The non-persistent notches were introduced into the specimens using a water-jet technique. Shaunik et al. [19] examined how cracks propagate in concrete specimens featuring one, two, or three non-persistent joints when subjected to uniaxial compression. To create the non-persistent joints, aluminum blades were positioned into the molds and fixed at both the top and bottom. Mohammadi et al. [20] prepared rectangular, double-layered laboratory specimens composed of alternating hard and soft layers. In each specimen, two vertical notches with lengths of 20, 40, and 60 mm, respectively, were introduced in the same direction..This study aimed to examine how layer brittleness, bedding orientation, and notch length affect both delayed and rapid fracture behavior of the specimens, along with an analysis of the associated acoustic emission (AE) events.

Amini et al. [21] employed a mold measuring 150 × 120 × 50 mm to examine the influence of multiple discontinuous notches on the fracture response of quasi-rock specimens. In this study, the discontinuous notches were formed by placing 1 mm thick steel plates within 50 mm thick plastic foam. Sarfarazi et al. [22] prepared gypsum specimens measuring 100 × 150 × 150 mm containing fractures and cavities to investigate the interaction between cavities and notches under uniaxial loading. Aluminum plates and cylindrical inserts were placed within plastic foam to form the desired cracks and cavities. Sarfarazi et al. [23] fabricated concrete specimens measuring 150 × 100 × 50 mm to examine the influence of discontinuous notches on the fracture response under uniaxial compression. Each specimen contained three non-persistent notches with a length of 20 mm, oriented at different angles relative to the inclined faces, and was subjected to uniaxial loading. Fu et al. [24] prepared rock-like specimens (gypsum) measuring 150 × 150 × 50 mm to examine the influence of pre-existing non-persistent discontinuous notches on the failure mechanisms under U-shaped cutters. The specimens contained one or two notches with a length of 20 mm, oriented at 0°, 45°, and 90°. The distances of the cracks from the top of the mold were controlled at 20 mm and 40 mm, respectively.

Mortezaei et al. [25] Laboratory specimens measuring 200 × 240 × 50 mm, consisting of soft and hard gypsum layers with pre-defined notches of 20, 40, and 60 mm in length, were prepared to examine the influence of layer orientation and brittleness on shear fracture response (Figure 2).

Chen et al. [26] designed and fabricated rock-like specimens containing a circular cavity along with a set of non-persistent notches to examine the effect of these notches on the stability of underground openings and the mechanical behavior of the specimens under uniaxial compressive loading (Figure 3).

Chen et al. [27] fabricated rock-like specimens with dimensions of 200 × 200 × 200 mm using a water: cement: sand mass ratio of 1:2:3. Parallel notches at different orientations were introduced in the specimens to replicate natural rock formations, and shear tests were conducted under various normal stress levels. The study investigated the effect of crack orientation and normal stress magnitude on crack propagation paths, failure mechanisms, and the shear strength of the specimens (Figure 4).

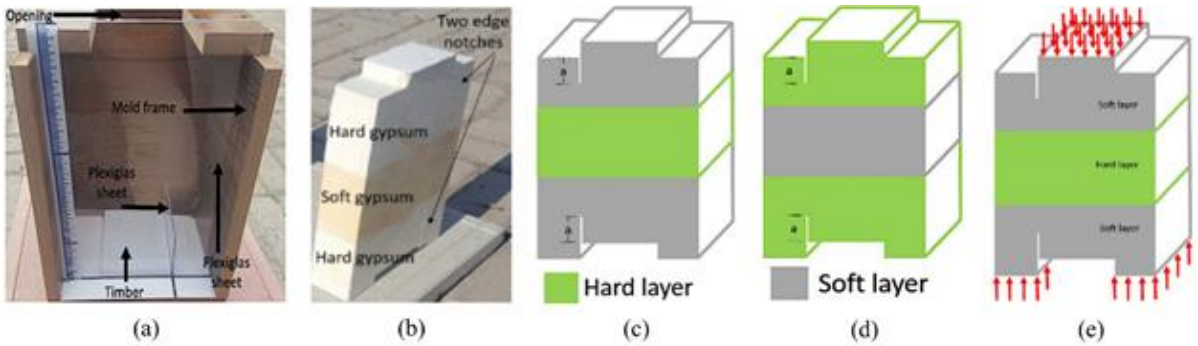

Figure 2. (a) MDF mold, (b) fabricated notched layered sample, (c) three-layer configuration incorporating a hard interlayer, (d) three-layer configuration incorporating a soft interlayer, and (e) a notched bedding layer subjected to a punch shear test [25].

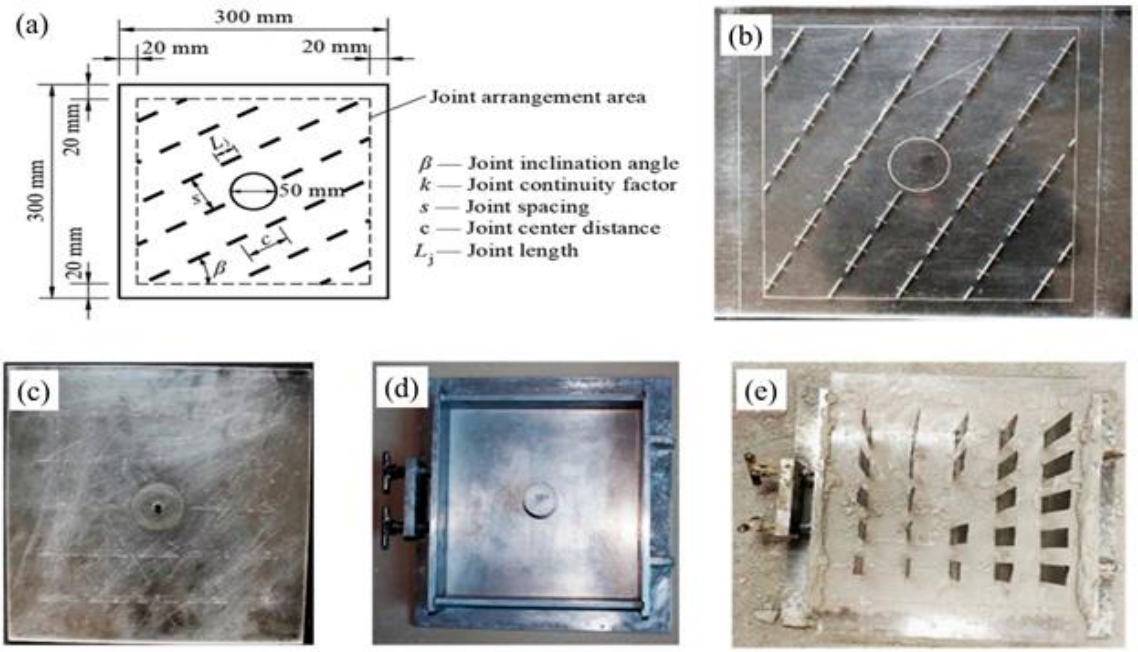

Figure 3. Overview of the mold and fabrication procedure for a sample: (a) dimensional specifications and joint-set geometry, (b) the cover plate, (c) the base plate, (d) the frame assembled with the base plate and the cylinder, and (e) a sample before solidification [26].

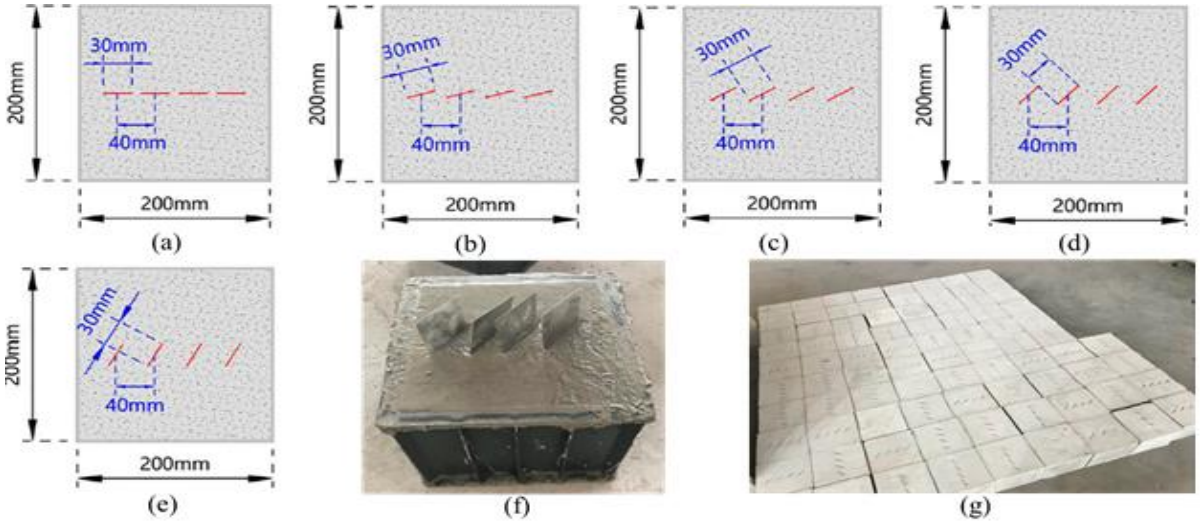

Figure 4. Schematic representation of a rock sample containing parallel joints joint groups: (a) joint inclination of 0°, (b) joint inclination of 15°, (c) joint inclination of 30°, (d) joint inclination of 45°, (e) joint inclination of 60°, (f) sample after joint pre burial, and (g) Finished models [27].

Sarfarazi et al. [28] prepared laboratory gypsum specimens with dimensions of 200 × 200 × 50 mm. Each specimen contained one to three non-persistent notches with a fixed length of 6 cm, and the crack orientations relative to the horizontal axis were varied from 0° to 90°. The study aimed to examine the effect of the number and orientation of notches on the fracture response and uniaxial compressive strength of the specimens (Figure 5).

Shemirani et al. [29] fabricated gypsum specimens in the laboratory with dimensions of 120 × 120 × 50 mm. Vertical grooves were introduced at the four corners of each specimen, and the specimens were prepared with three different notch configurations: parallel in-plane, inside echelon, and outside echelon, with varying notch lengths of 2, 4, and 6 cm. This study aimed to examine the influence of notch bridge length and orientation on the shear behavior and failure mechanisms of the specimens (Figure 6).

Haeri et al. [30] in this study fabricated specimens using two types of mixtures: the first type consisted of water and gypsum with a ratio of 0.6, and the second type consisted of water, sand, and cement with weight proportions of 27%, 33%, and 40%, respectively. The designed physical models included two lateral layers of concrete with dimensions of 160 × 130 × 60 mm and a central gypsum layer with dimensions of 16 × 13 × 6 mm. In these models, two horizontal joints were embedded in the concrete layers, and an inclined joint was introduced in the gypsum layer (Figure 7).



Figure 5. (a) Placement of the frame (200 mm × 200 mm × 100 mm) together with a specialized plastic fiber insert (200 mm × 200 mm × 50 mm) and the shim positioned inside the fiber, (b) alignment of the wooden box within the frame, (c) positioning of the shim inside the frame, and (d) slurry filled into the box [28].

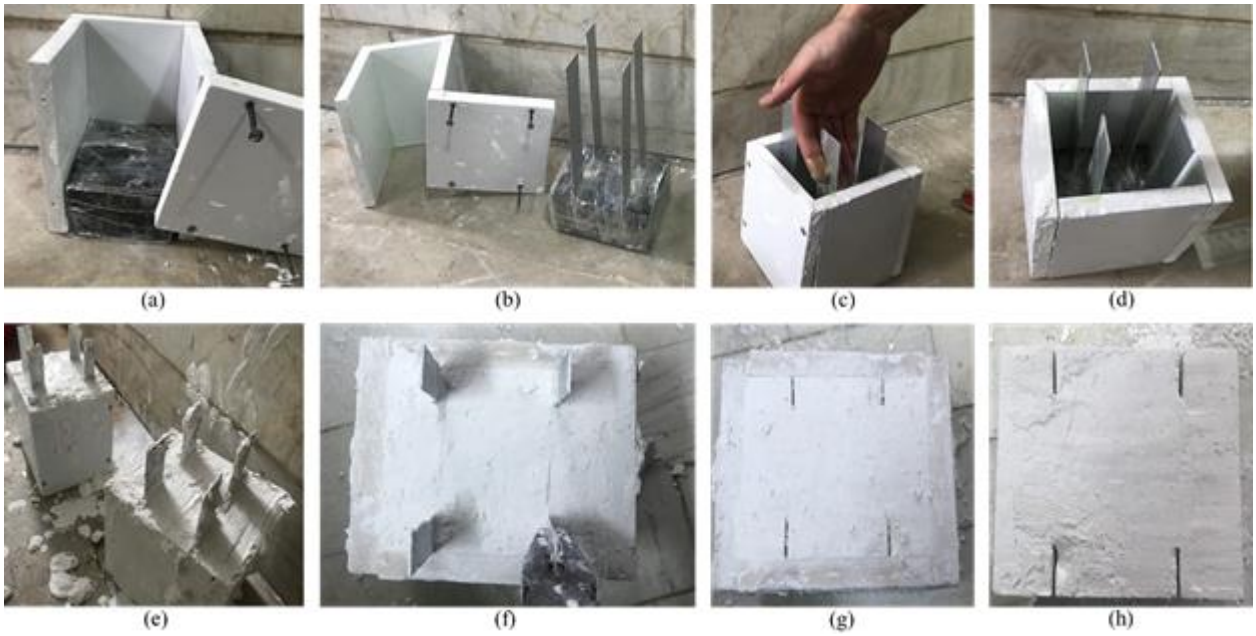

Figure 6. (a) Placement of a specialized black plastic fiber insert (10 cm × 10 cm × 5 cm) into the frame, (b) positioning of the shim within the plastic fiber, (c) application of grout around the shim, (d) adjustment of the shim inside the frame, (e) pouring of plaster slurry into the mold, (f) removal of the aluminum sheet from the mold, (g) specimen with a non-persistent crack retained in the frame, and (h) specimen with a non-persistent crack after removal from the frame [29].

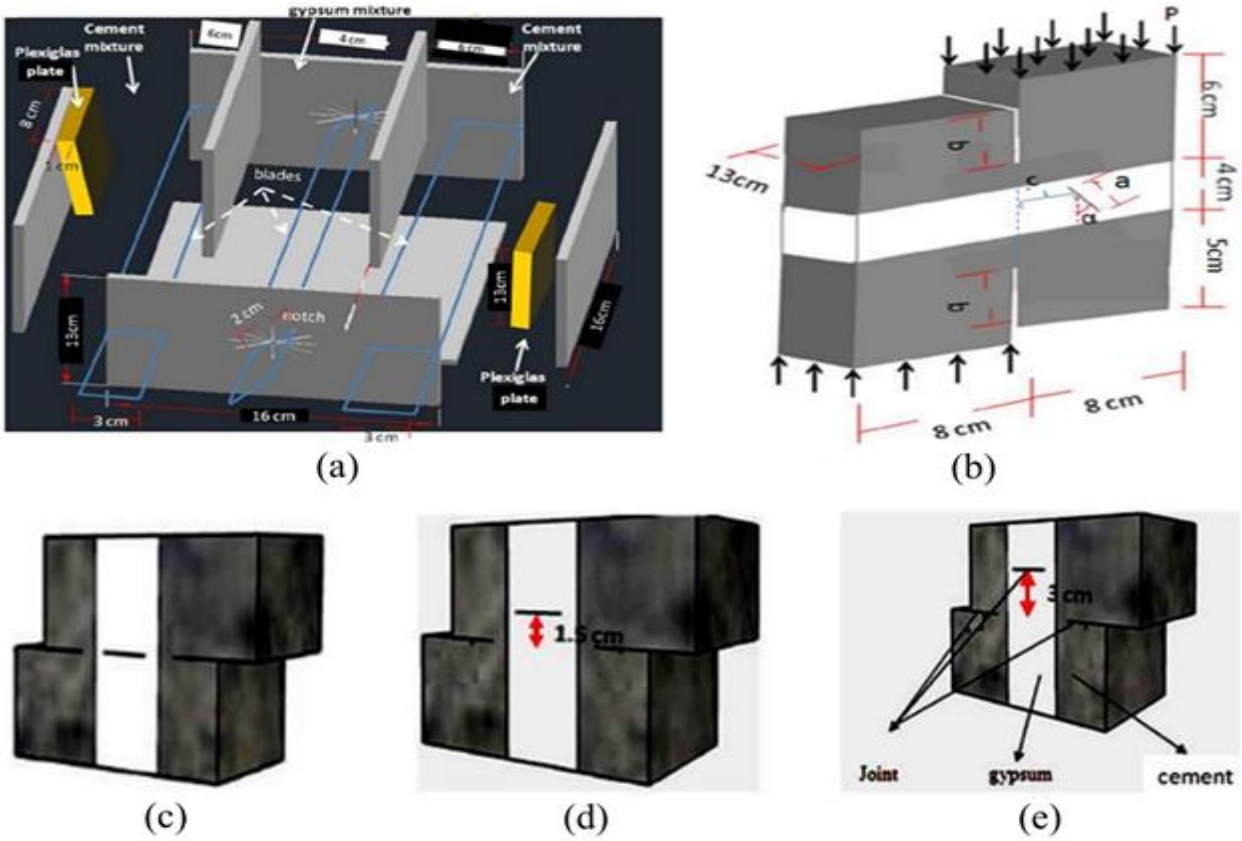

Figure 7. (a)The special mold consisting blades, mixture plates and Plexiglas plate, (b) model geometry, Central joint is placed (c) along the vertical edge joints, (d) at the distance of 1.5 cm from the central joints, and (e) at a distance of 3 cm from the central joints [30].

Mortezaei et al. [31] prepared heterogeneous rock-like laboratory specimens using MDF molds with dimensions of 250 × 200 × 50 mm and gypsum–water mixtures with varying ratios. The purpose of this specimen preparation was to create non-persistent notches within the samples. To form the grooves, various methods were evaluated, including the placement of aluminum blades, water jet cutting, use of diamond wire, and manual sawing (Figure 8).

Pan et al. [32] prepared cylindrical siltstone–sandstone specimens with a height of 100 mm and a diameter of 50 mm from the Linhuan coal mine in Anhui Province. Some of the specimens contained pre-existing notches with a length of 30 mm, a thickness of 4 mm, and an inclination of 30°, while others were intact. Triaxial tests were conducted using a Rock600-50 apparatus under varying confining pressures (0, 8, 16, 24, and 30 MPa) with displacement-controlled axial loading. Concurrently, specimen deformation and acoustic emission (AE) signals were monitored until complete failure (Figure 9).

Mohammadi et al. [33] developed laboratory specimens using various layered models. These models included a single soft layer, a single hard layer, a two-layer model consisting of one hard and one soft layer, a three-layer model with an intermediate soft layer, and a four-layer model comprising two hard and two soft layers. In all specimens, two edge notches were introduced in a single direction (Figure 10).

Wang et al. [34] prepared rock-like specimens by employing a mixture of cement, fine sand, and water in a mass ratio of 3.9:3.7:1.515 in steel molds measuring 150 × 150 × 50 mm. To create pre-existing notches, two steel plates with a thickness of 0.5 mm were placed in parallel at specified positions, forming notches with a 45° inclination, 25 mm length, and 0.5 mm width within the specimens. After 28 days of curing and surface preparation, uniaxial compression tests were conducted at different loading rates, accompanied by acoustic emission (AE) monitoring to evaluate the mechanical characteristics of the specimens and examine the damage–failure development model (Figure 11).

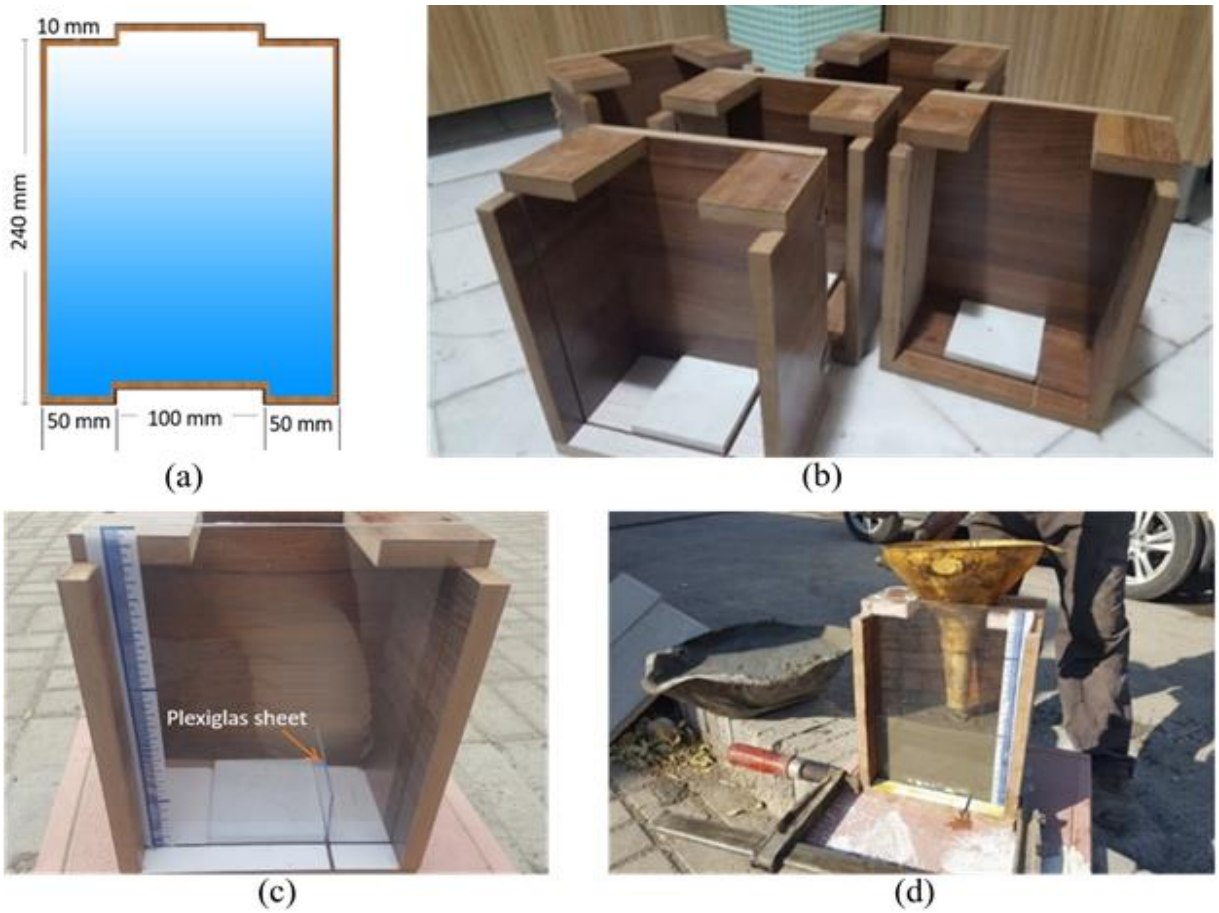

Figure 8. (a) Schematic illustration of the mold, (b) MDF mold, (c) notch at the base of the mold with a plexiglass sheet inserted, and (d) sequential pouring of slurry into the mold [31].

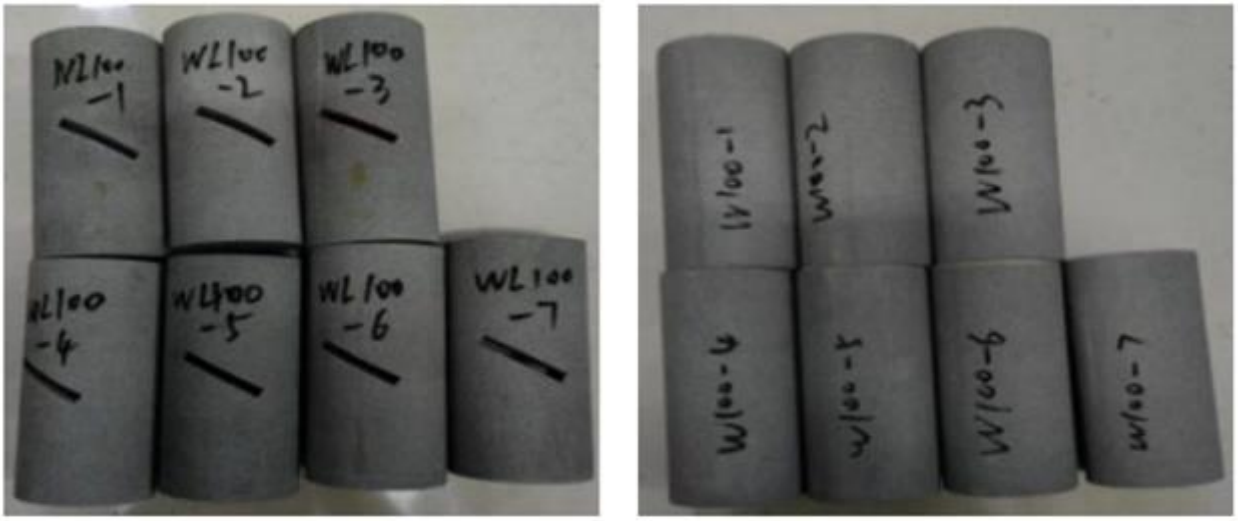

Figure 9. Prefabricated cracks and preparation of complete specimens [32].

Sarfarazi et al. [35] The specimens were prepared using a cement–water mixture with a mass ratio of 2:1. T-shaped non-persistent joints were introduced by inserting thin metal sheets into the fresh cement paste and withdrawing them after solidification. The notch lengths were set to 1, 2, 3, 4, and 6 cm, with inclination angles of 0°, 30°, 60°, 90°, 120°, and 150°. Each specimen had a thickness of 40 mm and a diameter of 100 mm. After casting, the specimens were cured under cool and dry laboratory conditions for 28 days before testing (Figure 12).

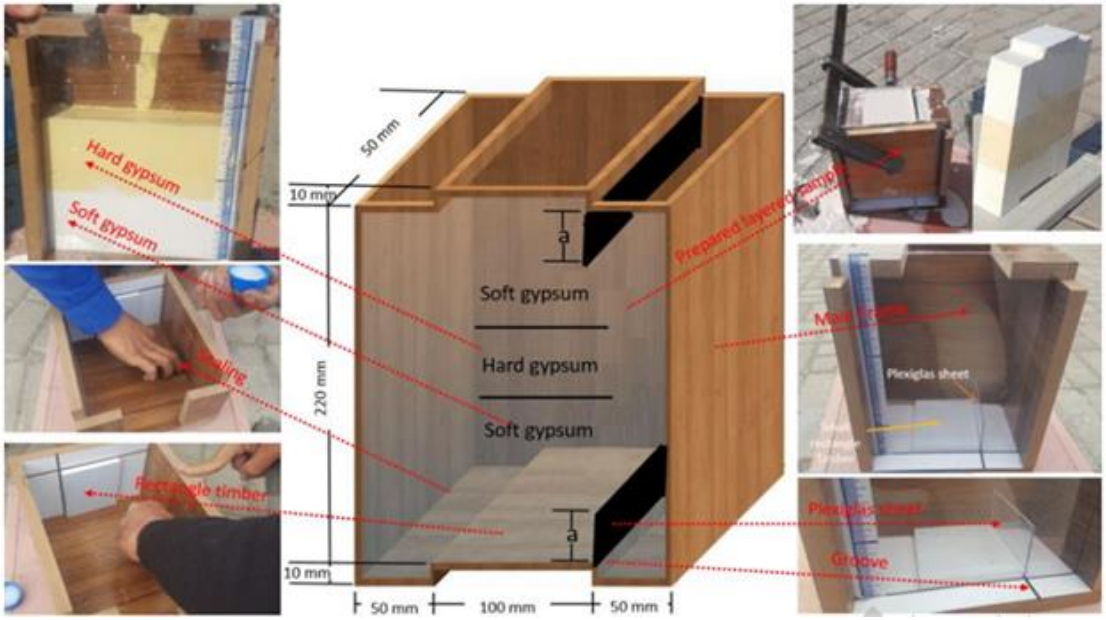

Figure 10. Sealed mold featuring a grooved timber base with a plexiglass sheet inserted into the groove [33].

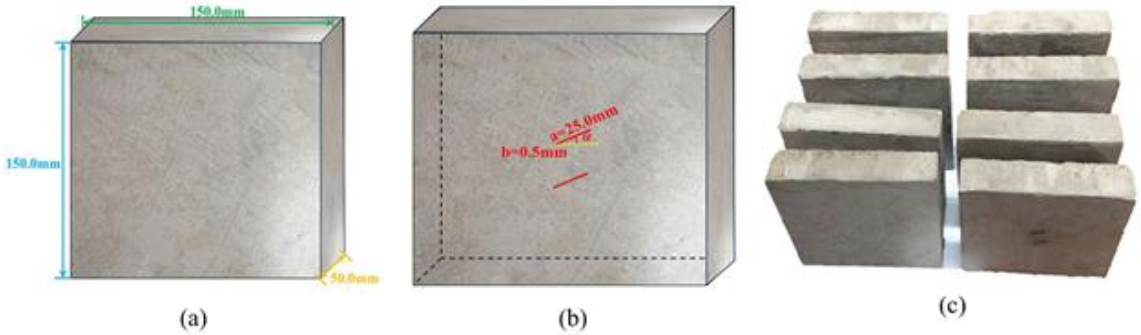

Figure 11. Diagram of specimen: (a) specimen parameters, (b) fissure parameters, (c) actual specimen [34].

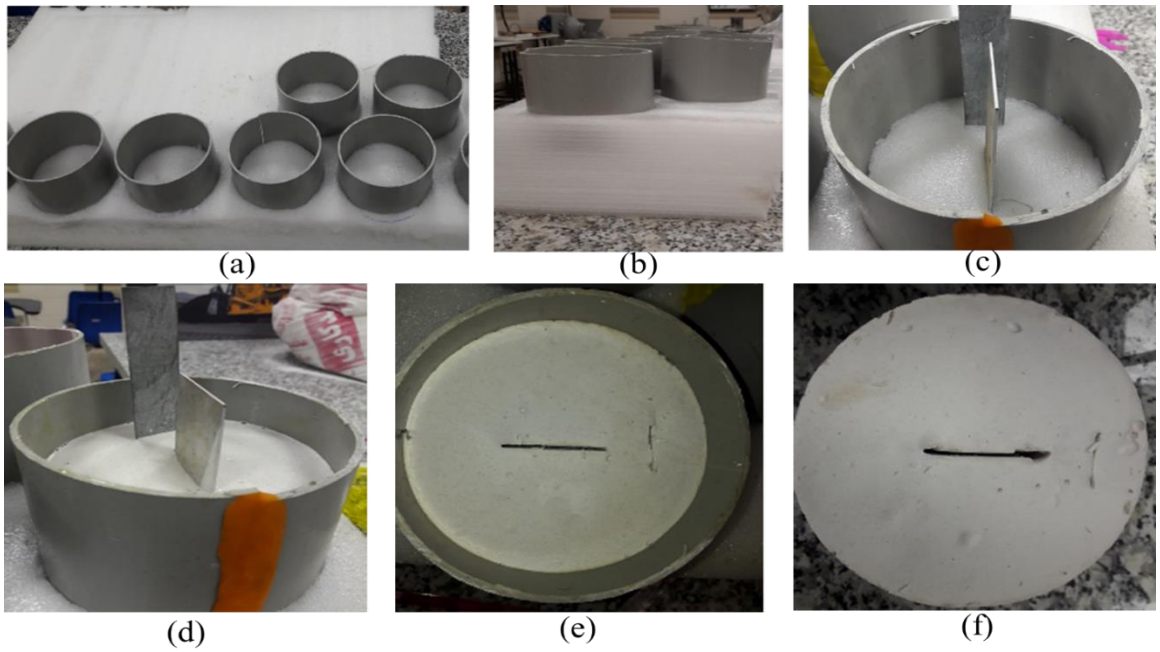

Figure 12. (a) Frame with a diameter of 10 cm and a thickness of 40 cm, (b) another view of the same frame, (c) placement of a 100 mm × 1 mm × 60 mm shim inside the plastic fiber, (d) plaster slurry poured into the mold, (e) removal of the aluminum sheet from the mold, and (f) specimen incorporating a T-shaped non-persistent joint [35].

Rezaei et al. [36] The specimens were produced by mixing gypsum and water at a mass ratio of 1.3:1 and casting them in cubic molds with dimensions of 70 × 70 × 50 mm. Edge notches were introduced by inserting thin plates into the molds, which were removed after initial hardening. The notch length was 10 mm, with inclination angles of 10°, 20°, and 30°. The samples were cured under cool and dry conditions for 14 days (Figure 13).

Sarfarazi et al. [37] To prepare the samples, plaster and water were mixed at a ratio of 1.5:1 (plaster/water). A stainless-steel mold with dimensions of 15 × 15 × 15 cm was filled with the mixture. Aluminum blades with 1 mm thickness and 20 cm length, bent at 2 cm from the top, were greased and inserted into the mold to simulate non-persistent joints and rock bridges. These blades allowed the formation of discontinuities occupying 0.2, 0.4, and 0.6 of the shear surfaces. After curing, the mold was removed, and cubic blocks with semi-continuous joints and rock bridges were obtained for mechanical testing (Figure 14).

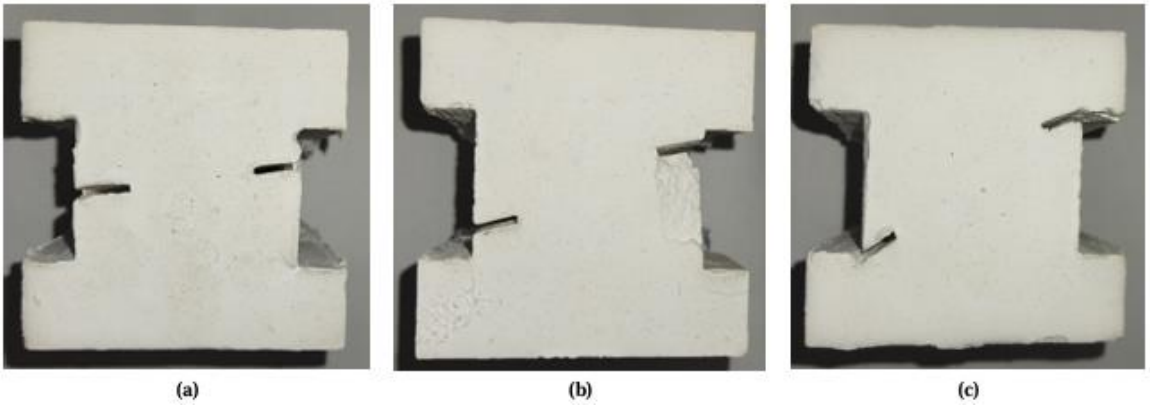

Figure 13. Edge-notched pillars featuring a 10 mm notch and notch angles of (a) 10°, (b) 20°, and (c) 30° [36].

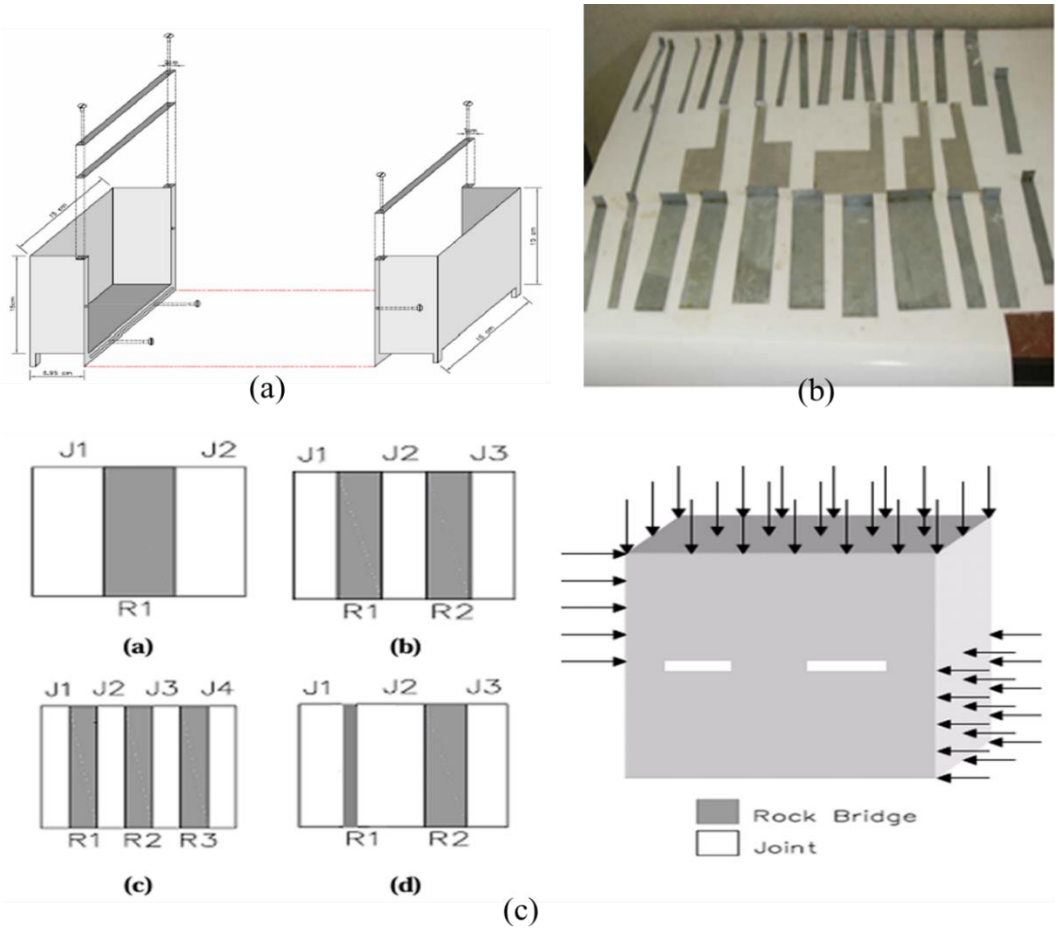

Figure 14. (a) Mold used for building the samples, (b) Sheets used in order to create joints in the rock bridge, and (c) Various rock bridge samples created for the test [37].

In previous studies, numerous investigations have been conducted on rock-like specimens containing non-persistent notches under uniaxial loading to characterize the fundamental mechanical characteristics and fracture patterns of rocks. These experiments, performed using natural or synthetic materials, have provided valuable insights into compressive and tensile strength, elastic modulus, and specimen behavior under controlled conditions. However, in many engineering applications, such as mining, slope design, and explosive loading, rocks are subjected to high strain-rate loading, which can induce fracture mechanisms and energy dissipation patterns that differ from those observed in static tests. Consequently, recent studies have focused on dynamic testing of specimens with pre-existing notches in rocks and rock-like materials to examine the influence of notches length, orientation, and number on dynamic behavior, progressive fracture, and energy distribution. This approach provides a more comprehensive understanding of the dynamic response of rocks and establishes a solid basis for designing the present experiments on magnetite iron ore specimens containing non-persistent edge notches.

Li et al. [38] This study examined the influence of pre-existing flaw geometry, including flaw length and orientation, on the dynamic mechanical behavior of marble. Specimens with dimensions of 60 × 60 × 15 mm were prepared, each containing a single artificial notch with a length of 10 mm and an approximate width of 1.4 mm. The notch orientation was varied across the specimens to enable a comprehensive analysis of fracture mechanisms. This study aimed to elucidate the relationship between notch geometric parameters and the dynamic response of the specimens under high strain-rate loading using the Hopkinson pressure bar test (Figure 15).

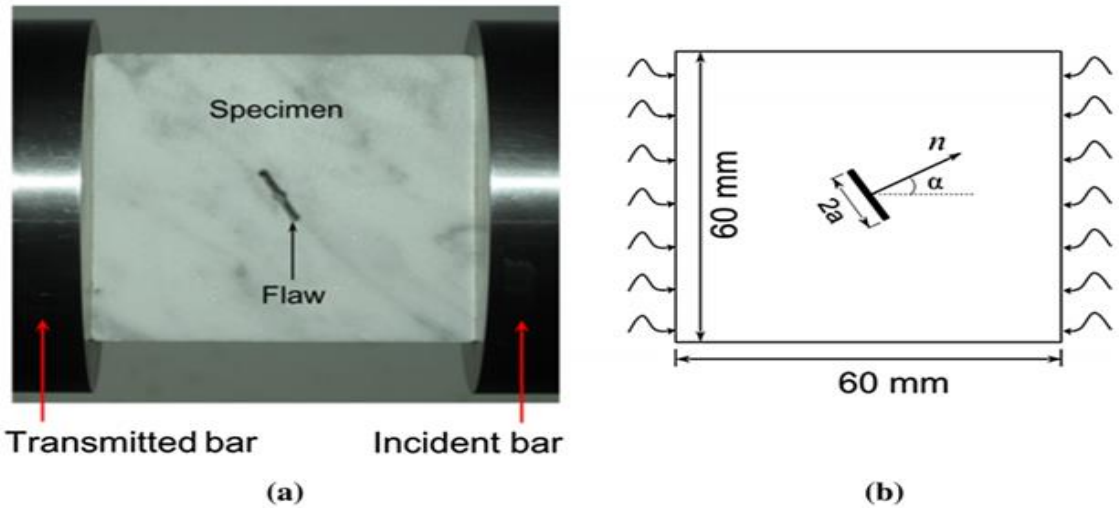

Figure 15. (a) Specimen positioned between the bars, and (b) schematic of a single-flaw marble specimen with flaw inclination angle α and half flaw length a = 5 mm. Loading is applied from right to left [38].

Yan et al. [39] This study examined the influence of crack intensity on the dynamic mechanical behavior of rock by preparing laboratory sandstone specimens in a cuboid shape with dimensions of 45 × 35 × 35 mm. To simulate different discontinuity conditions, specimens were fabricated with one, two, and three pre-existing parallel cracks. Each crack had a length of 7 mm, a width of 1 mm, and was oriented at 45° relative to the loading direction, with a fixed spacing of 8 mm between cracks. This design aimed to evaluate the role of crack number and geometry in the fracture process and the dynamic response of the specimens under high strain-rate loading (Figure 16).

Yan et al. [40] prepared cuboid sandstone specimens with dimensions of 35 × 35 × 45 mm to examine the mechanical response of multi-flawed samples under combined static–dynamic loading and progressive fracture mechanisms. Each specimen contained several pre-existing flaws with a length of 7 mm, a width of 1 mm, and a fixed spacing of 8 mm. The flaw orientations were designed in four configurations (15°, 30°, 45°, and 60°) to systematically evaluate the effect of non-persistent flaw orientation on the fracture process and the evolution of damage (Figure 17).

Zhao et al. [41] prepared laboratory granite specimens with dimensions of 45 × 45 × 20 mm, each containing two parallel pre-existing notches

with a length of 10 mm, a width of 1 mm, and a thickness of 1 mm. The notches were oriented at various angles of 0°, 45°, and 90° relative to the horizontal to systematically examine the influence of the influence of notch angle and intensity on the dynamic behavior, fracture mechanisms, fragmentation characteristics, and energy dissipation of the specimens under impact loading in SHPB tests (Figure 18).

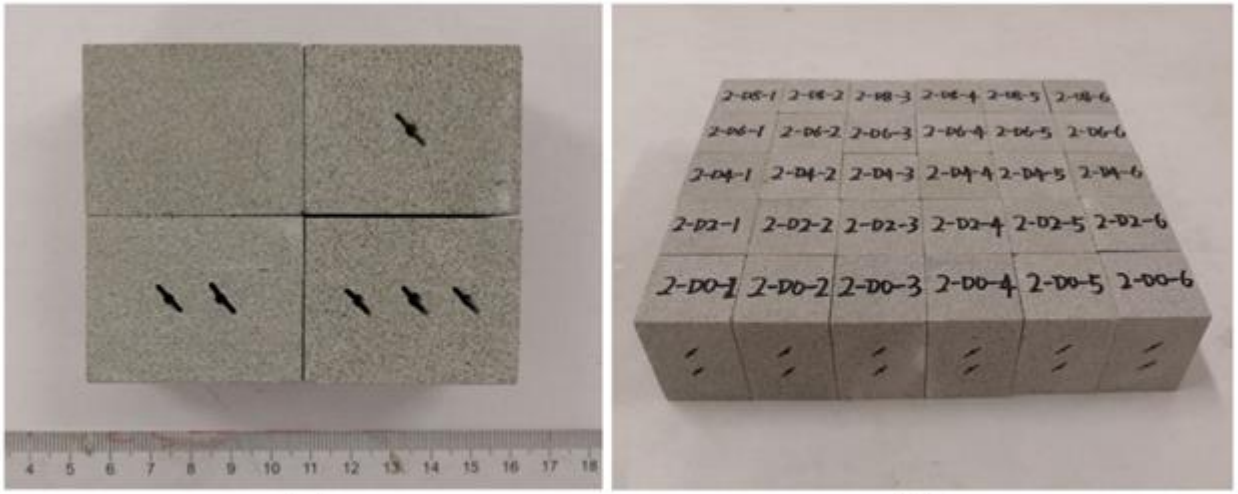

Figure 16. (a) Four categories of pre-cracked rock specimens with different crack intensities, and (b) assembled parts of specimens ready for SHPB experiments [39].

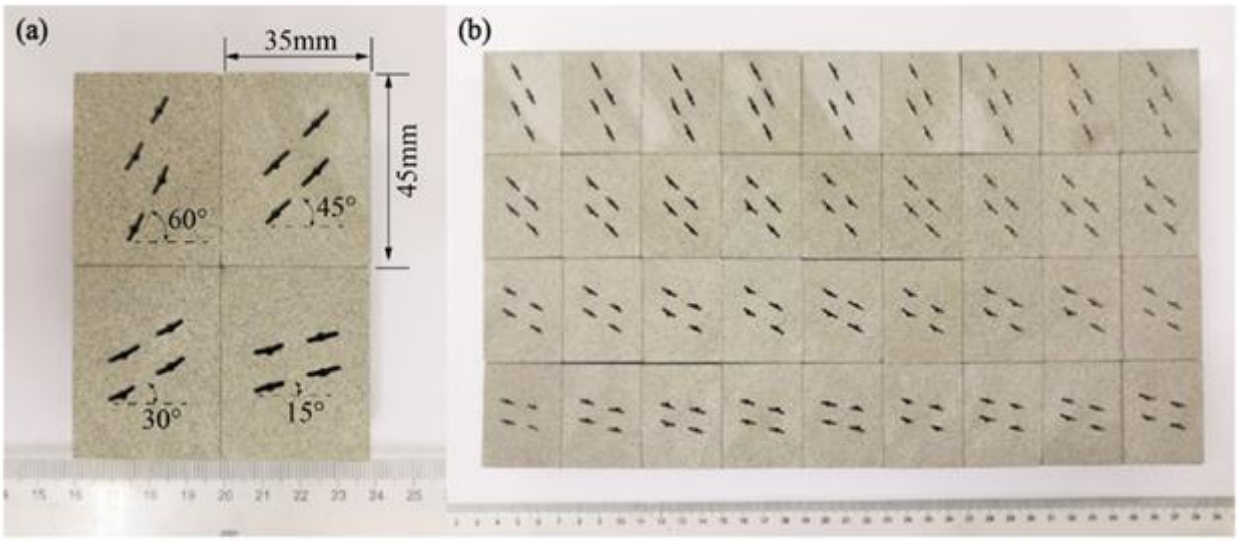

Figure 17. (a) Schematic representation of the geometry of multi-flawed rock specimens, and (b) specimen components prepared with different flaw inclination angles [40].

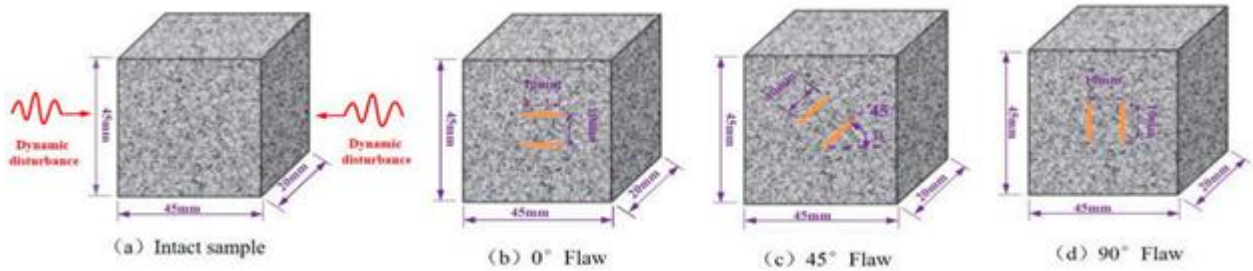

Figure 18. Geometrical images of the specimens [41].

Wang et al. [42] prepared laboratory plate-like quasi-rock specimens with dimensions of 47 × 47 × 15 mm by employing a mixture of cement, fine sand, and water in a weight ratio of 1:3:0.57. Each specimen contained two types of pre-existing flaws: open cracks and flaws filled with epoxy resin. The flaw length was set at 6 mm, and the flaw angles were varied from 0° to 90° in 15° increments. This design aimed to examine the effect of flaw angle and type on the dynamic strength, fracture mechanisms, and stress distribution of the specimens under impact loading in SHPB tests (Figure 19).

Kumar et al. [43] Cubic quasi-rock specimens with an edge length of 34 mm using a mixture of artificial stone powder (Dental die stone), fine Ennore sand, and water in a weight ratio of 12:1:2.88. to examine the influence of discontinues notches and notch -filling conditions on dynamic mechanical behavior and fracture patterns, a single pre-existing notch with a length of 10 mm, a width of 2 mm, and an inclination angle of 30° was introduced in the notched specimens. Furthermore, some specimens were deliberately filled with cement or epoxy resin to enable a comparative examination of the effect of filling conditions on the dynamic response (Figure 20).

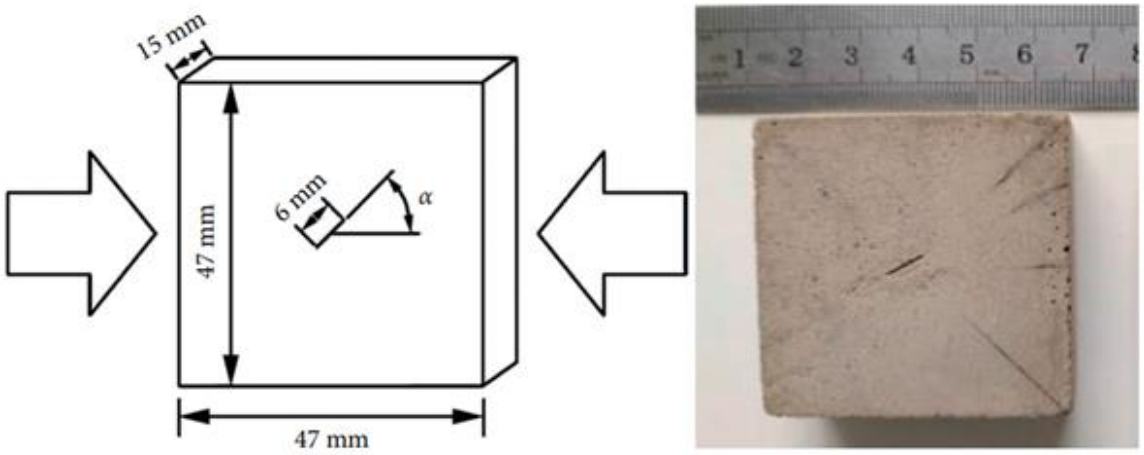

Figure 19. Configuration of a specimen containing a single flaw [42].

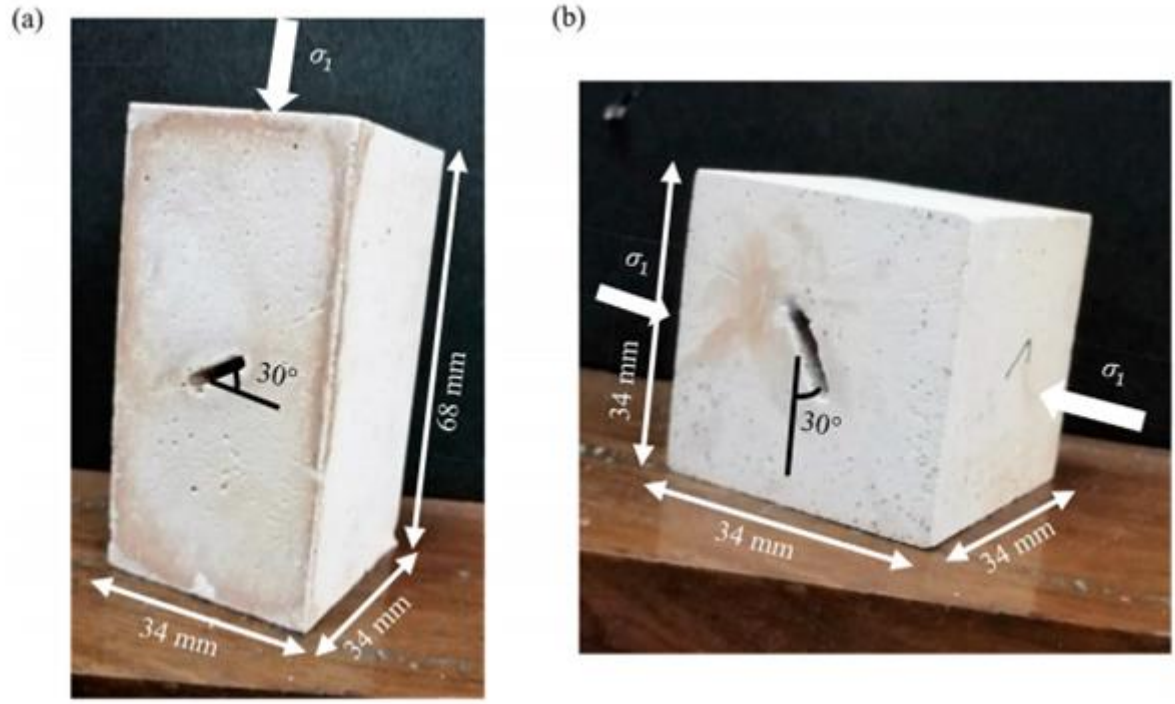

Figure 20. Sample specifications for (a) static uniaxial compression testing and (b) dynamic SHPB compression testing [43].

Lei et al. [44] Laboratory specimens of red sandstone with dimensions of 46 × 30 × 15 mm were prepared to examine the influence of pre-existing notch angles on the mechanical behavior of notched samples under both static and dynamic loading. A single pre-existing notch with a length of 8 mm was introduced at the center of each specimen, and its orientation relative to the specimen's longitudinal axis was set at 0°, 30°, 45°, 60°, and 90°. The specimens were subjected to uniaxial compression and impact loading tests using a Split Hopkinson Pressure Bar (SHPB) apparatus. (Figure 21).

Ji et al. [45] prepared laboratory sandstone specimens with dimensions of 50 × 50 mm. A pre-existing rectangular notch measuring 16 × 1 mm was introduced in each specimen to examine the effect of notch orientation on the dynamic response under high strain-rate loading (Figure 22).

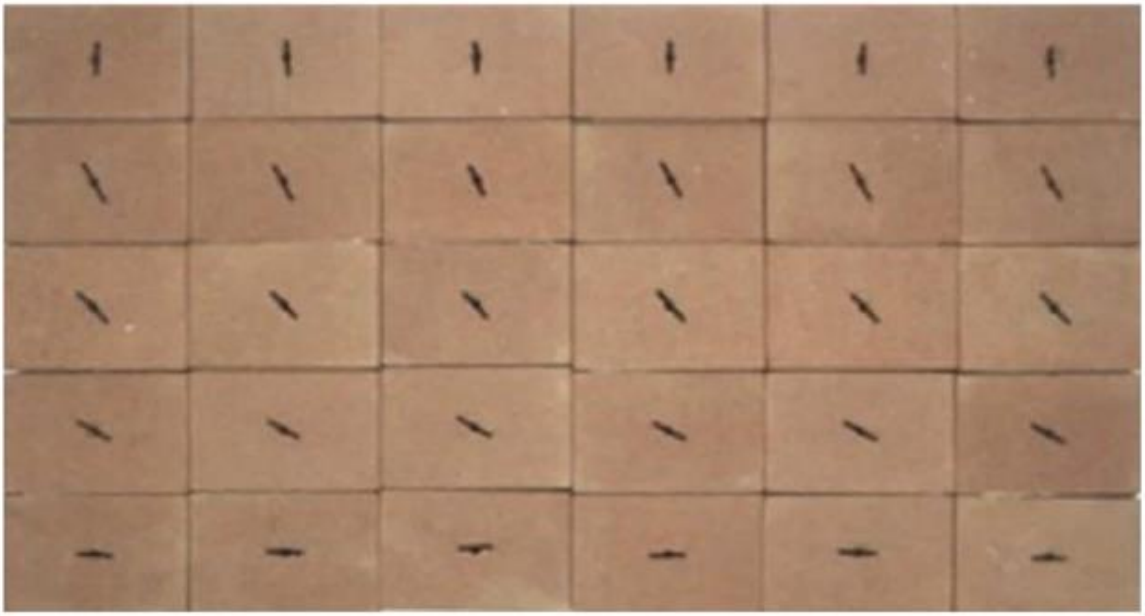

Figure 21. A part of samples [44].

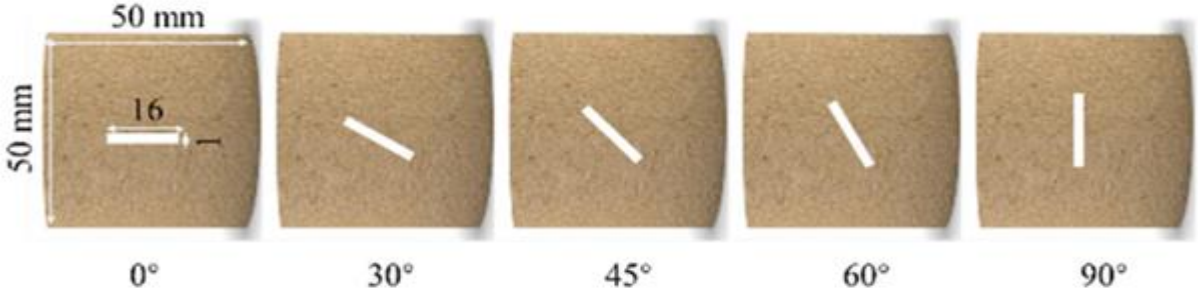

Figure 22. Samples with different angles [45].

Zhou et al. [46] prepared laboratory specimens of white sandstone with dimensions of 45 × 45 × 15 mm. A pre-existing notch measuring 8 mm in length and 1 mm in width was introduced at the center of each specimen. The notches were oriented at angles of 0°, 30°, 45°, 60°, and 90° relative to the horizontal to examine the effect of notch orientation on the dynamic response and fracture mechanisms under high strain-rate loading using the SHPB apparatus (Figure 23).

Ping et al. [47] prepared laboratory specimens of sandstone with a diameter and height of 50 mm. A pre-existing flow measuring 20 mm in length, 2 mm in width, and oriented at 45° was introduced in each specimen. Prior to testing, the specimens were submerged in water for 48 hours to achieve full saturation. These specimens were then used to examine the dynamic mechanical characteristics and fracture behavior under impact loading using the SHPB apparatus (Figure 24).

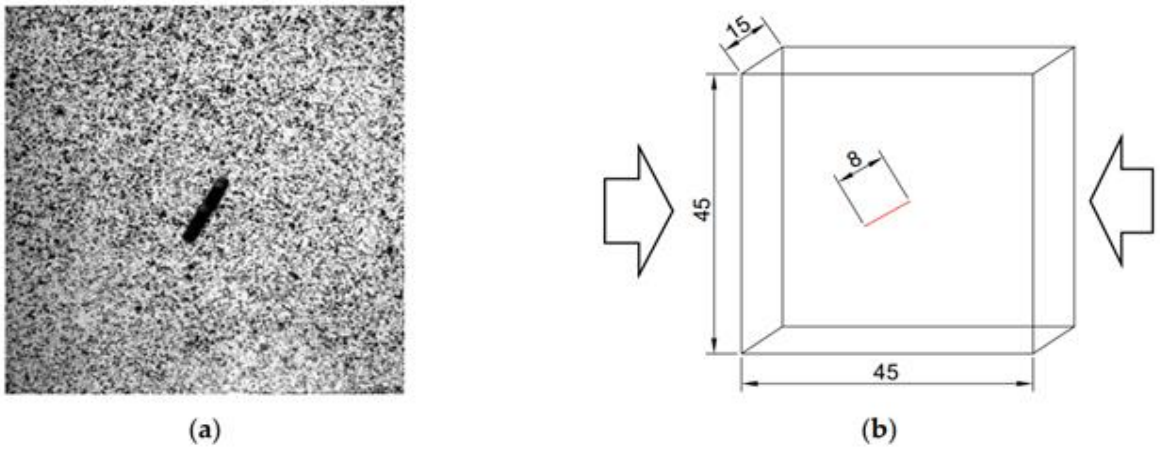

Figure 23. Illustration of speckle pattern application and dynamic loading: (a) specimen, and (b) loading diagram [46].

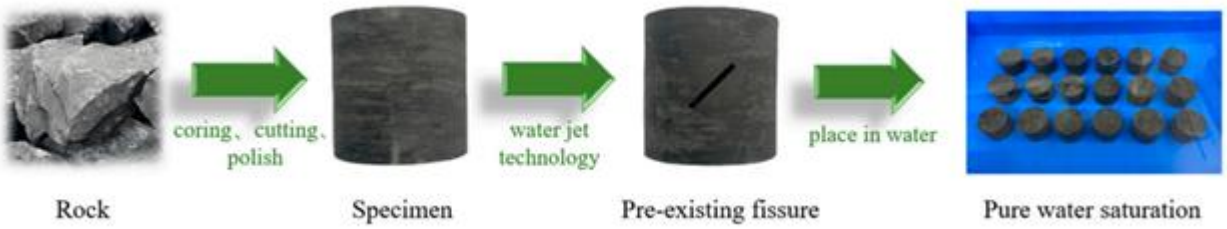

Figure 24. Flowchart illustrating the preparation of water-saturated fractured sandstone sample [47].

Yin et al. [48] prepared laboratory specimens of red sandstone with dimensions of 100 × 25 × 50 mm. Two pre-existing notches, each 1 mm wide, were introduced in each specimen: a vertical crack in the upper section and an inclined notch in the lower section. The crack lengths were varied at 50, 60, and 70 mm to simulate stone bridges, enabling a systematic to examine the effect of bridge length and moisture conditions on the dynamic mechanical characteristics, fracture mechanisms, and damage extent of the specimens (Figure 25).

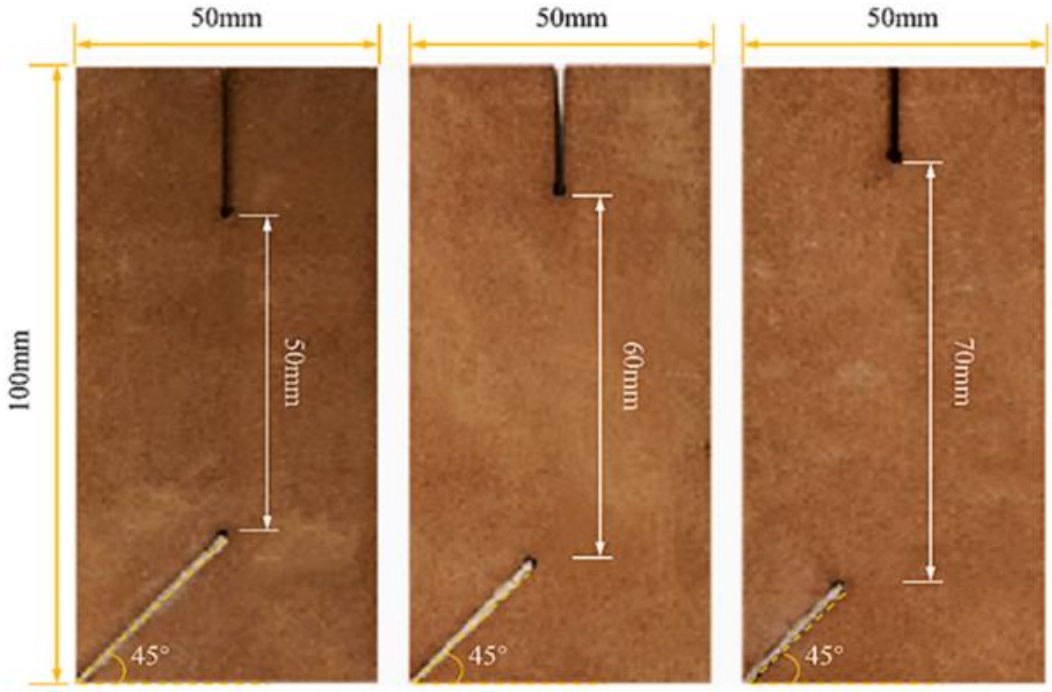

Figure 25. Dimension of defective specimen [48].

Zou et al. [49] The specimens were prepared by mixing Hydrocal B-11 gypsum, diatomaceous earth, and water at a weight ratio of 175:70:2. The mixture was cast into prismatic molds and, after hardening, dried in an oven at 40 °C. Two sizes of specimens were fabricated: normal specimens with dimensions of 152×75×32 mm, and small specimens with dimensions of 35×35×26 mm and 19×19×35 mm. Artificial single and double flaws were introduced by inserting metallic shims into the fresh gypsum paste parallel to the specimen thickness, which were removed after hardening. In double-flaw specimens, the geometry was defined by the flaw inclination angle (β), bridging length (L), and bridging angle (α) (Figure 26).

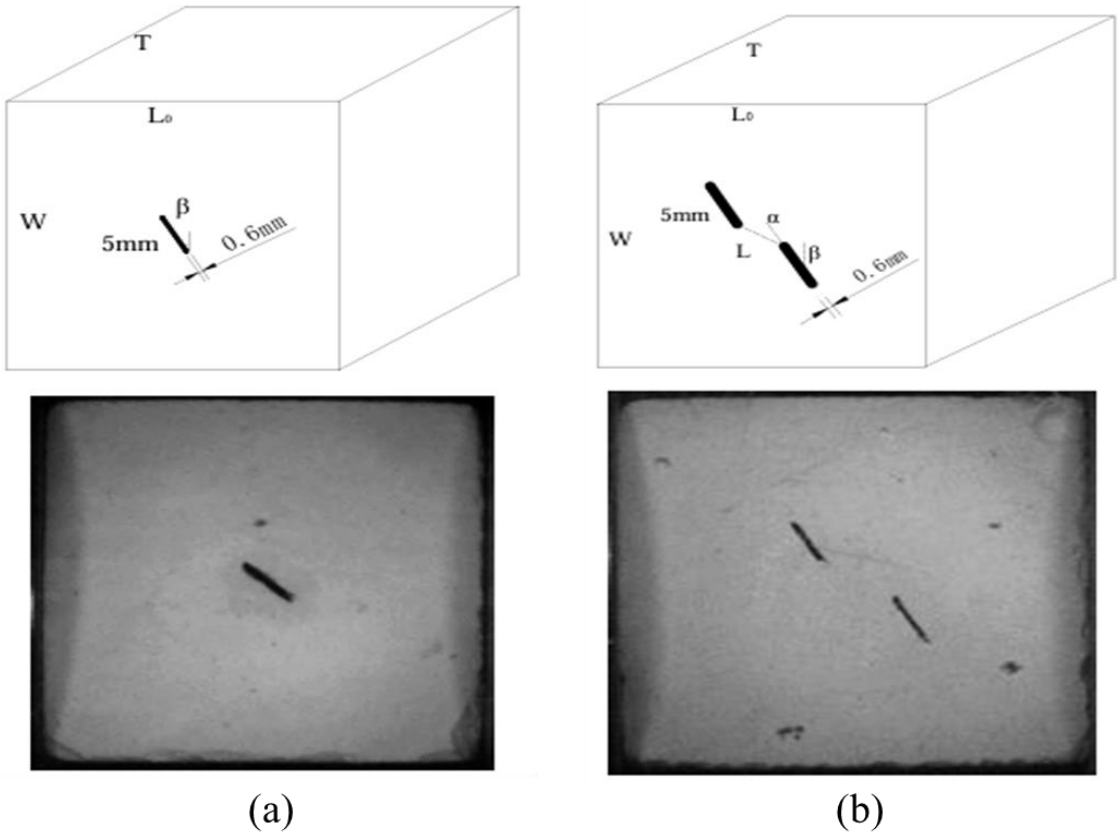

Figure 26. (a) Geometry of a small specimen with a single flaw, and (b) geometry of a small specimen with two flaws. L denotes the bridging length, α the bridging angle, and β the flaw inclination angle [49].

While the above studies focus on experimental specimen preparation, recent research has increasingly concentrated on modeling and analyzing contact mechanics in layered or functionally graded materials using analytical, numerical, and hybrid approaches. Numerous works have investigated the influence of material heterogeneity, layer interactions, and loading conditions on contact stress distribution and deformation behavior. For instance, Yaylaci et al. examined contact problems in functionally graded layers and orthotropic materials using analytical formulations, finite element analyses, and artificial neural network techniques [50–57]. These studies provide valuable insights into material responses under complex loading conditions and multi-method evaluations. Although such works primarily address numerical and analytical modeling rather than experimental specimen preparation, they contribute to a broader understanding of mechanical behavior that can guide the design of laboratory-scale physical models for uniaxial compression and fracture testing.

Despite extensive studies on quasi-rock specimens under uniaxial and dynamic loading, there remain gaps in understanding the actual dynamic behavior of mineral rocks containing pre-existing notches. In the present study, for the first time, cylindrical iron ore specimens extracted from the Galali open-pit mine were prepared with non-persistent edge notches under dry, saturated, and frozen conditions, featuring varying notch lengths, angles, and positions. These specimens enable the investigation of the combined effects of notch angle, length, and position on dynamic response,

progressive fracture processes, and energy distribution, addressing the limitations of previous studies that primarily focused on quasi-rock or artificially fabricated samples. Moreover, this study provides a standardized methodology for preparing natural rock specimens for high strain-rate dynamic testing using the Hopkinson Pressure Bar. In this approach, selected rock blocks were cored into standard cylindrical specimens, and non-persistent edge notches of varying lengths and angles were introduced to simulate natural heterogeneities. Specimens were conditioned under various environmental states—dry, saturated, and frozen—to examine the influence of environmental conditions on their mechanical response. The results obtained in this study can serve as a practical guide for the preparation of real rock specimens in laboratories and contribute to improved accuracy and enhanced reliability of mechanical testing.

2. Materials and Methods

2.1 Rock Sampling and Selection

In this reserch, iron ore blocks were collected from the Galali open-pit mine. Blocks with varying shapes and geometries were selected to assess the effectiveness of coring and the quality of the extracted cores from each block, as well as to determine the number of cores obtainable from each block. To maintain structural and mineralogical homogeneity, all cores were extracted from a single parent block.

At the mining site, each block was visually and meticulously evaluated to ensure the absence of large natural joints, weathered zones, and non-uniform mineral veins that could compromise the structural integrity of the specimens. The selected blocks were extracted using conventional drilling-and-blasting techniques, which are standard mining practices in the Galali open-pit mine. This extraction method ensures controlled fragmentation while preserving the integrity of the blocks selected for coring. The extracted blocks were then immediately sealed in impermeable plastic bags to prevent moisture changes and mechanical damage during transportation to the laboratory.

This approach preserves the natural characteristics of the rock and ensures specimen uniformity for subsequent experimental procedures. Figure 27 provides an overview of the extracted blocks and the selected specimens prepared for coring.



Figure 27. Selected specimens at the mine site.

2.2 Core Drilling of Specimens

After transporting the extracted blocks to the laboratory, the core drilling process was initiated. Two different core diameters were considered for specimen preparation:

- 54 mm diameter for uniaxial and Brazilian tests
- 22 mm diameter for dynamic testing using the Split Hopkinson Pressure Bar (SHPB)

The selection of these two diameters was based on the specific technical requirements of the tests. The larger 54 mm specimens are suitable for quasi-static uniaxial compression and Brazilian tensile tests because they minimize boundary effects and

provide more reliable measurements of bulk mechanical properties. In contrast, the 22 mm cores were prepared for SHPB testing because smaller specimens are necessary to achieve high strain rates and ensure one-dimensional stress wave propagation. Therefore, the use of two different diameters reflects the distinct experimental requirements of static and dynamic loading conditions.

Diamond-tipped drills were used for coring, and a continuous flow of cooling water was maintained throughout the process to minimize friction and heat generation, thereby preventing microcracks and surface damage to the cores.

During drilling, ensuring the parallel alignment of the drill axis with the block surface was crucial. Any misalignment between the drill surface and the core, or incomplete contact of all drill teeth with the rock, could lead to localized stress concentrations and an increased risk of segment failure (Figure 28). Therefore, precise adjustment of the drill angle relative to the block surface was essential to preserve the structural integrity of the cores.

Precise control of the coring speed was also of critical importance, as deviations from the optimal range could cause significant issues in both sample quality and equipment performance. Specifically, excessively high coring speeds led to the failure of diamond segments, potentially resulting in the drill becoming stuck within the rock (Figure 29a). Conversely, excessively low speeds increased wear on the core barrel walls and produced surface irregularities on the samples, thereby compromising the quality and structural integrity of the extracted cores (Figure 29b). Therefore, selecting and maintaining an appropriate coring speed is essential for preventing equipment damage and ensuring the reliability and accuracy of laboratory test results.

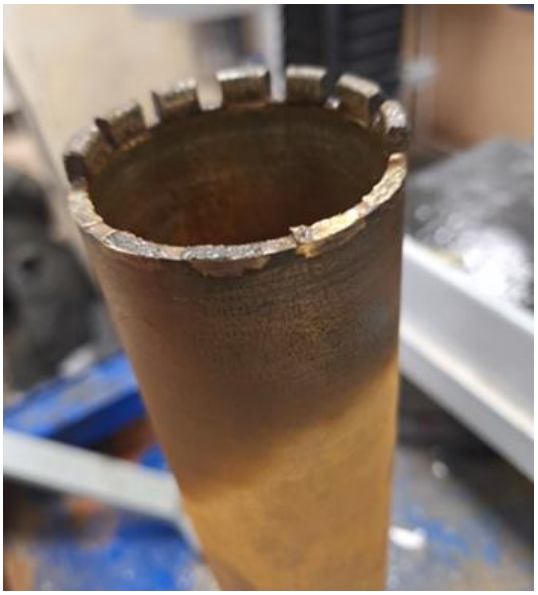

Figure 28. Segment failure due to incomplete contact of all drill teeth with the rock surface.



(a) (b)

Figure 29. Effect of coring speed on core quality: (a) high speed, and (b) low speed.

After the coring process was completed, all extracted cores underwent a thorough quality inspection to ensure the absence of internal cracks, potential structural defects, and surface irregularities. To assess the geometry and dimensional accuracy of the samples, the initial length and diameter of each core were precisely measured and recorded. These measures ensured the selection of intact and homogeneous specimens for subsequent mechanical testing stages (Figure 30).

2.3 Geometric Preparation of Samples

After the coring process, the samples were precisely cut using a precision cutter to achieve standardized dimensions suitable for each type of test (Figure 31). The sample preparation strictly adhered to the geometric requirements of the respective tests, as follows:

- Uniaxial Compression Test: cores with a diameter of 54 mm and a height of 108 mm (Figure 32-a);
- Brazilian Test: cores with a diameter of 54 mm and a height of 27 mm (Figure 32-b);
- Dynamic SHPB Test: cores with a diameter of 22 mm and a height of 22 mm (Figure 32-c).

All dimensions and geometric ratios were selected and implemented based on the guidelines provided by the International Society for Rock Mechanics (ISRM) to ensure comparability and reproducibility of the experimental results.



(a) (b)

Figure 30. Extracted core samples with varying diameters: (a) 54 mm diameter cores for uniaxial and Brazilian tests, and (b) 22 mm diameter cores for dynamic testing.

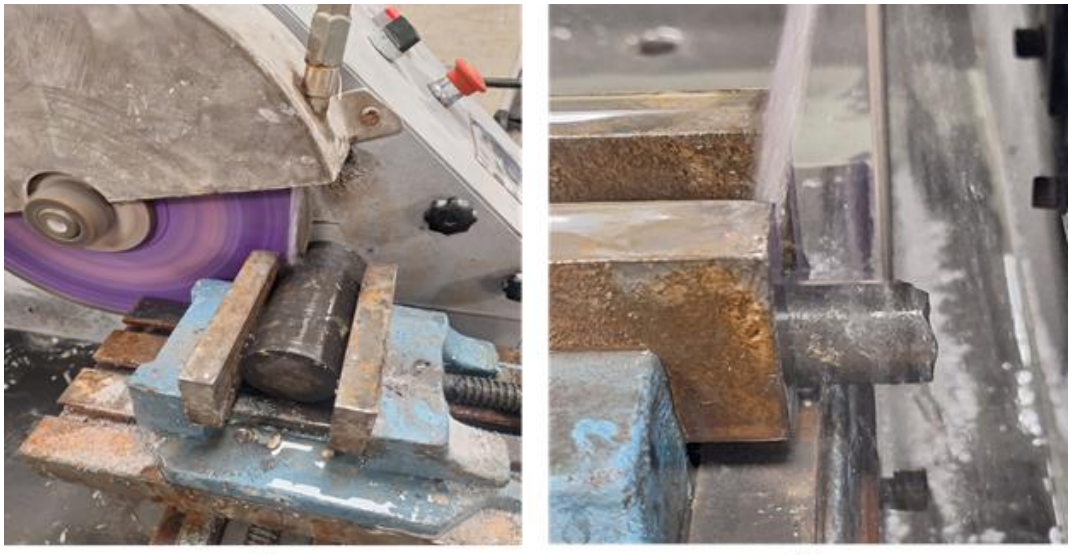

(a) (b)

Figure 31. Cutting of specimens with different diameters: (a) 54 mm, and (b) 22 mm

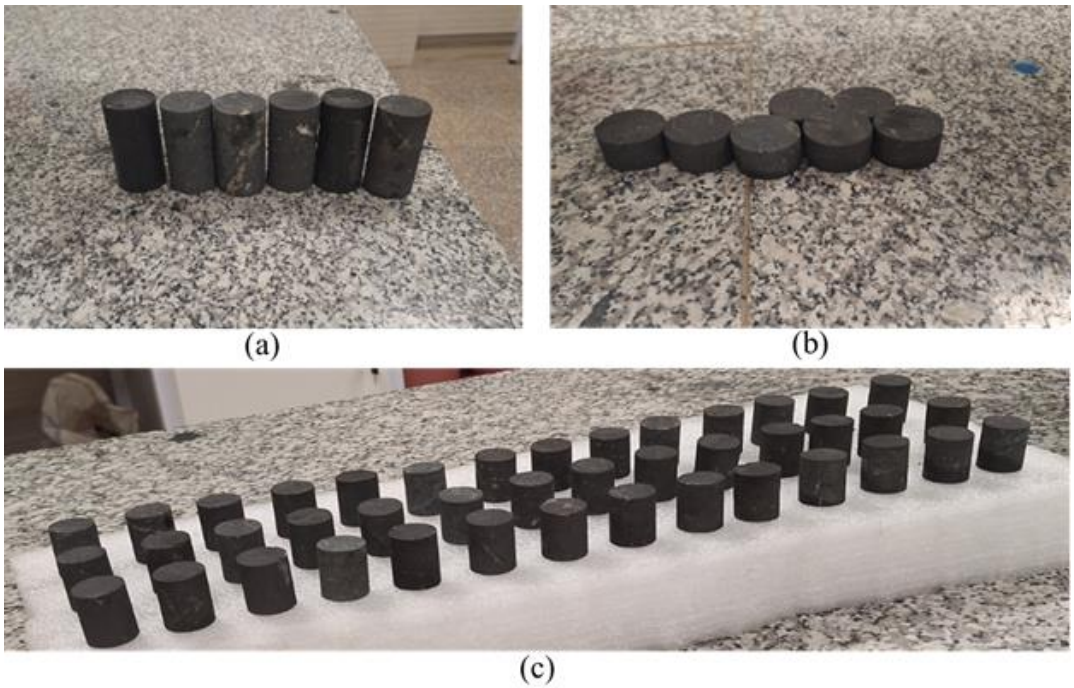

Figure 32. Prepared core samples for different tests: (a) uniaxial compression, (b) Brazilian tensile, and (c) dynamic SHPB tests

The top and bottom faces of the cores were subsequently ground and polished using abrasive sand and silica powder to ensure complete flatness, parallelism, and coplanarity, while minimizing surface roughness. This process was conducted to guarantee the accuracy and repeatability of mechanical test results and to prevent stress concentrations during loading. The geometric tolerances maintained during this stage were as follows:

- Deviation from flatness of end surfaces: ≤ 0.02 mm;
- Non-parallelism of end surfaces: ≤ 0.001 rad;
- Surface roughness: Ra ≤ 1.6 μm.

These values were selected and applied in accordance with international standards for rock sample preparation (Figure 33).



Figure 33. Polishing and parallelization of the samples: (a) application of silica powder, and (b) ensuring the levelness of the sample surface.

Finally, two different methods were employed to prepare ice samples for the uniaxial and Brazilian tests:

Method 1: In this approach, four uniaxial and four Brazilian rock samples were first coated with a thin layer of grease and placed on a foam mold. Greased blades were used to separate the samples, and the assembly was then placed into individual molds. The inner space of the molds was filled with a gypsum slurry (gypsum-to-water ratio of 0.5). After approximately three hours, once the gypsum had hardened, an attempt was made to remove the rock samples from the molds so that the resulting voids could be filled with water to produce ice samples. However, due to the brittleness and low mechanical strength of the gypsum, the molds fractured during sample removal, and this method failed (Figure 34).

Method 2: To overcome the limitations of the first method, plastic tubes with standard lengths and diameters corresponding to the uniaxial and Brazilian tests were used. The inner and outer surfaces of the tubes were coated with grease to prevent adhesion. The tubes were then placed in dedicated containers, with foam underneath to ensure a flat and smooth bottom surface, and the containers were filled with water (Figure 35a). However, due to the lower density of the foam compared to water, the tubes floated during filling. To resolve this issue, the foam was removed in the final stage, and the upper and bottom surfaces of the tubes were covered with thin greased plastic sheets. After freezing, this procedure produced smooth, parallel, and uniform ice surfaces. This method was successful, and ice samples of suitable quality for the experiments were obtained (Figure 35b).

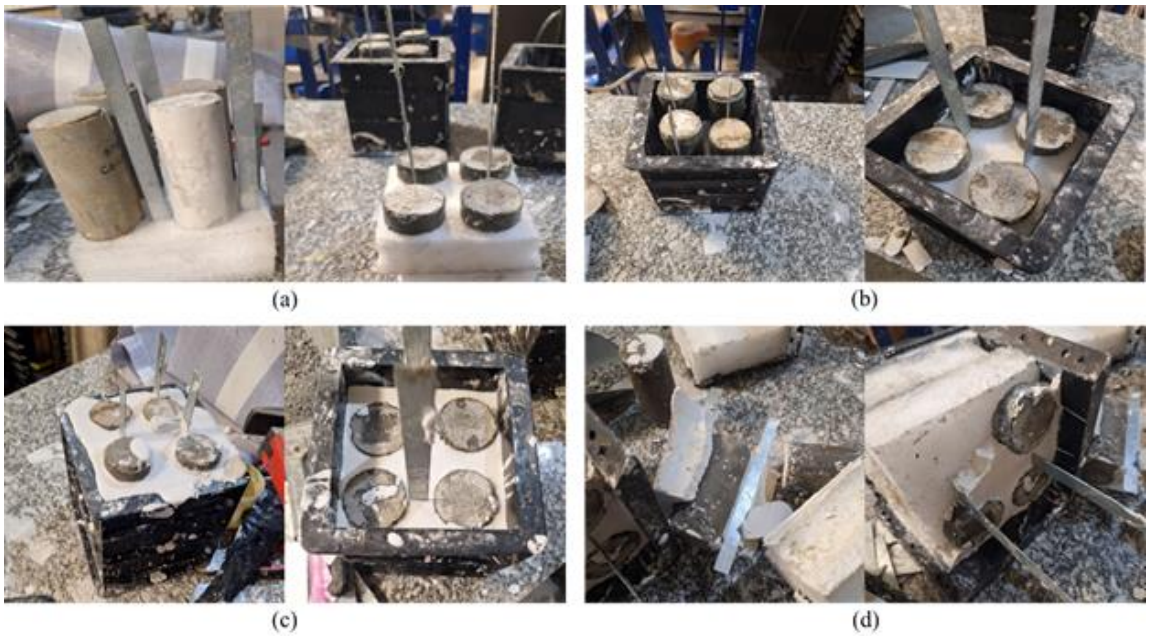

Figure 34. Ice sample mold preparation process: (a) placement of uniaxial and Brazilian rock samples on the foam mold, (b) positioning the samples within the box, (c) pouring gypsum slurry into the mold, and (d) removal of the rock samples from the mold.

2.4 Edge Notch Formation

After sample preparation, non-persistent edge notches were introduced into the dynamic specimens to simulate internal heterogeneities and natural fracture patterns in the rock. The geometric characteristics of these notches were defined as follows:

- Notch thickness: 3 mm;
- Notch angle relative to the dynamic loading axis: 0°, 30°, 60°, and 90°;
- Notch length: 20%, 40%, and 60% of the total specimen length.

Furthermore, to investigate the effect of notch location, different positions were considered for two specific angles:

- At 0°: notches were positioned at one-third, one-half, and two-thirds of the specimen height;
- At 90°: notches were placed separately in the top and bottom sections of the specimens.

To ensure precise notch formation, a diamond saw was mounted on an adjustable fixture to accurately control both the notch angle and length. Following cutting, all specimens underwent geometric quality inspection to confirm that the notch length, depth, and angle fully matched the design specifications. Specimens exhibiting chipped edges, surface irregularities, or deviations from target dimensions were discarded, ensuring that only intact and standardized samples were selected for dynamic testing (Figure 36).

For geometric inspection, digital calipers with 0.01 mm resolution were used to measure notch length and depth, and a digital protractor was employed to verify the notch angle. Notch length and depth were accepted if within ±0.1 mm of the target value, and notch angles within ±1° of the design angle. Specimens failing to meet these criteria or exhibiting chipped or irregular edges were rejected and replaced, ensuring that only fully compliant samples were used for testing.

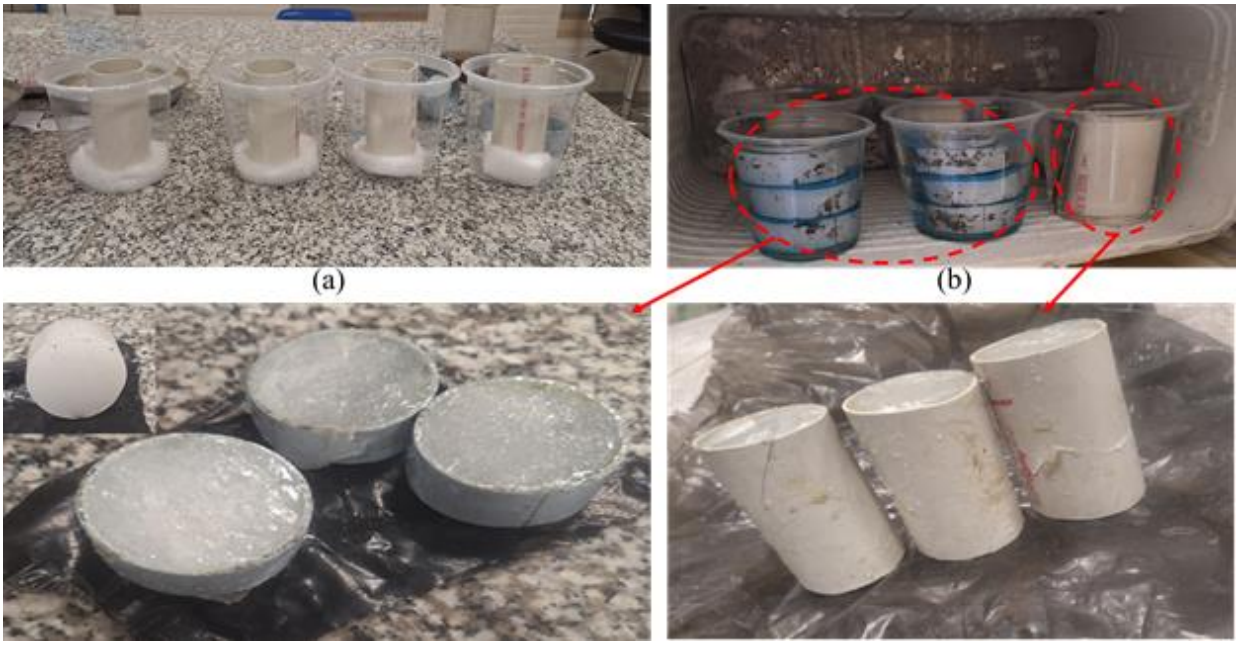

Figure 35. Ice specimens preparation steps: (a) placement of foam beneath the tubes in the containers, and (b) covering the upper and lower faces of the tubes with thin polyethylene sheets.

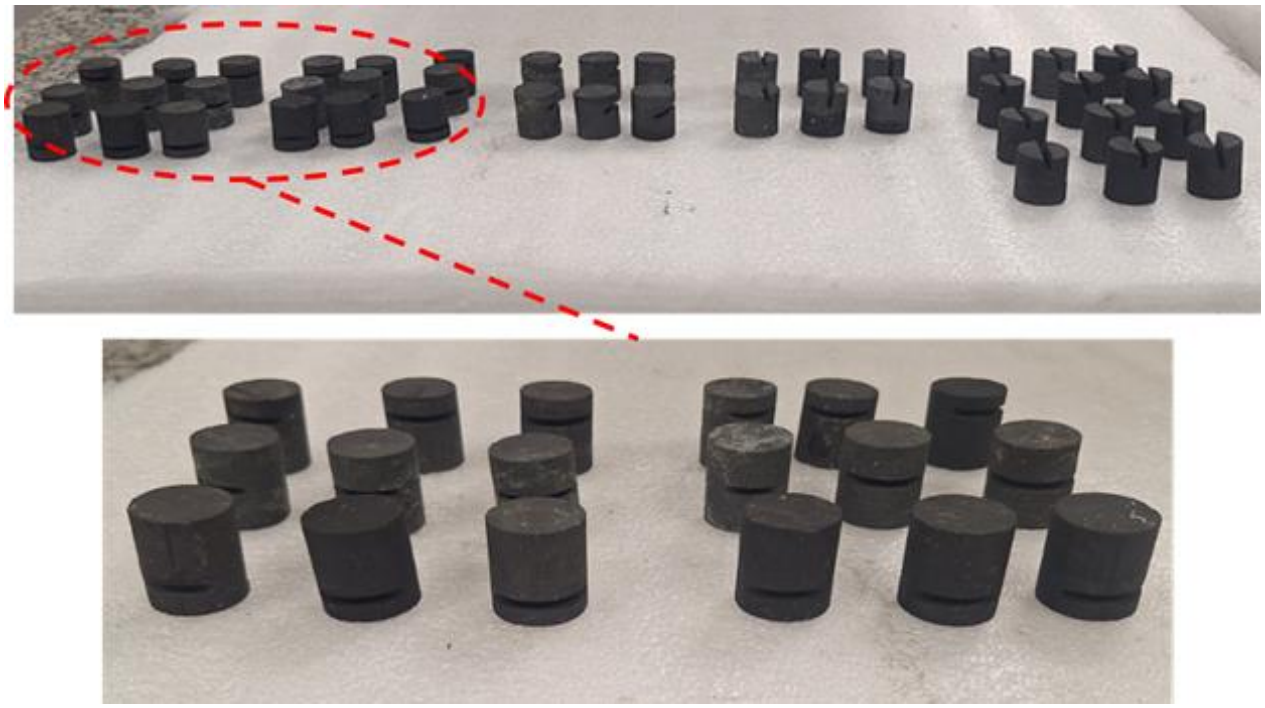

Figure 36. Core specimens containing non-persistent edge notches

2.5 Environmental Conditions of the Specimens

After the creation of the non-persistent edge notches, the specimens were divided into two separate groups:

- Dry group: comprising 21 specimens;
- Saturated and frozen group: comprising 21 specimens.

All 42 specimens were initially weighed to record their initial mass.

Dry condition:

Specimens in the dry group were placed in an oven at 70 °C for 24 hours to ensure complete drying. Upon completion of the drying process, the specimens were weighed again to verify the mass difference before and after drying. This step was conducted to ensure uniform moisture content and to eliminate the effect of free water on the mechanical response of the specimens (Figure 37).



Figure 37. Oven used for drying the specimens

Saturated and Frozen Conditions:

The specimens in the saturated group were first immersed in water for 48 hours to achieve complete saturation (Figure 38). After this step, the specimens were weighed to record the final saturated mass. An allowable mass difference of ≤0.5 % was considered acceptable to confirm the stability of the dry, saturated, and frozen conditions. To create frozen conditions, the edge-notched cracks of the specimens were exposed to a temperature of −5 °C for 24 hours, allowing the water within the cracks to solidify. Prior to testing, the specimens were re-weighed and inspected to ensure no unwanted cracking had occurred and that the ice had not melted.

Two different methods were tested for filling the cracks with ice:

Method 1: The specimens were coated with grease, leaving only the edge-notched cracks exposed. Each specimen was then placed individually in a container, and water was poured over it to fully submerge the cracks (Figure 39a). The specimens were kept in a freezer at −5 °C for 24 hours. However, upon removal, it was observed that the surrounding ice did not fully separate from the specimen, and the ice within the cracks fractured, preventing proper crack filling (Figure 40).

Method 2: To overcome the limitations of Method 1, cylindrical tubes with diameters matching the specimens were used. The saturated specimens were placed inside these tubes, which were then filled with water (Figure 39b). After 24 hours in a freezer at −5 °C, it was observed that only the water inside the cracks froze, resulting in correct and intact crack filling without damaging the specimen structure (Figure 41).

This second method successfully produced frozen specimens with accurately filled and stable cracks, making them suitable for subsequent dynamic testing.

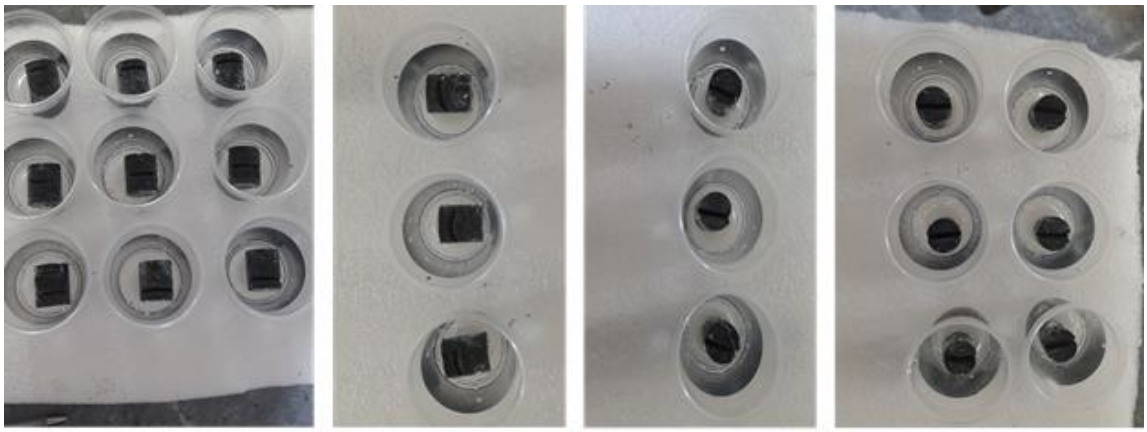

Figure 38. Saturated specimens with non-persistent edge notches at various angles: (a) 0°, (b) 30°, (c) 60°, and (d) 90°.



Figure 39. Stages of filling the notches with ice: (a) specimens placed in containers with diameters larger than the samples, and (b) specimens placed in tubes with diameters equal to the sample diameters.

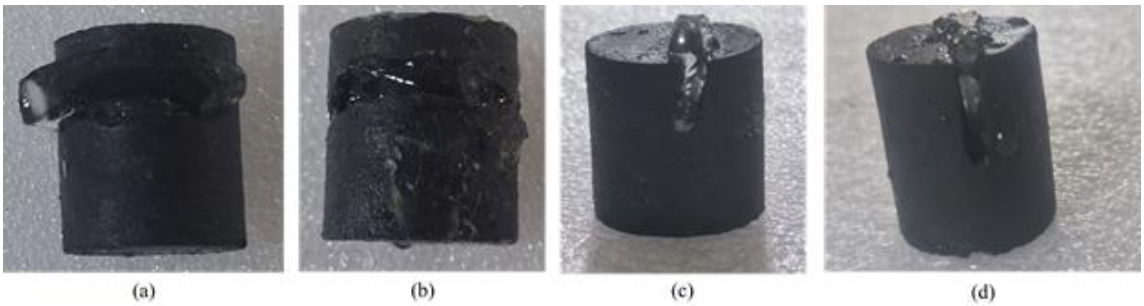

Figure 40. Improper ice filling of the notches at various angles: (a) 0°, (b) 30°, (c) 60°, and (d) 90°.

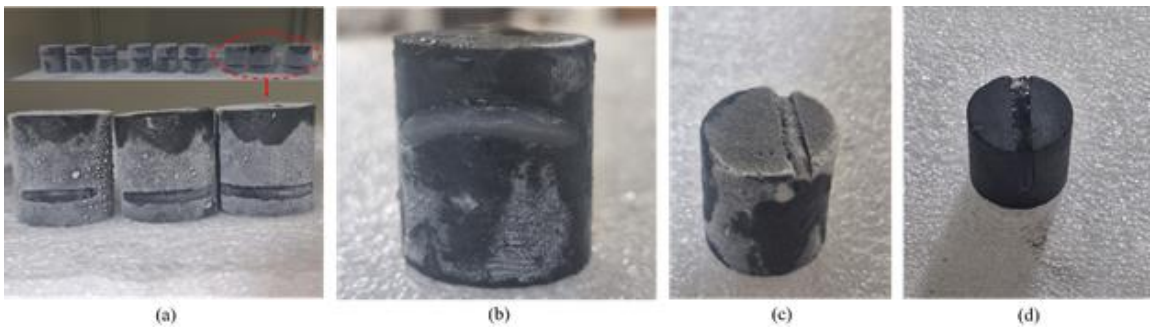

Figure 41. Proper ice filling of the notches at different angles: (a) 0°, (b) 30°, (c) 60°, and (d) 90°.

3. Discussion

In this study, the preparation process of iron ore specimens for uniaxial, Brazilian, and dynamic tests was comprehensively investigated. The results demonstrated that maintaining structural integrity and precise control over each preparation step prerequisites for obtaining reliable results. The selection of appropriate core diameters, ensuring the parallelism of the specimen axis, controlling coring speed, and employing continuous water cooling prevented core breakage and internal cracking, thereby ensuring the accuracy and comparability of experimental data.

Non-persistent edge notches were created with precise lengths, thicknesses, and angles, and specimens exhibiting chipping or irregularities were discarded to maintain uniformity and high precision. The specimens were conditioned under dry, saturated, and frozen states, with initial and secondary weights carefully recorded. For frozen specimens, the use of plastic tubes along with internal and external lubrication ensured smooth, uniform ice surfaces and prevented damage to the samples.

In addition to these standard procedures, three practical and innovative measures were implemented to enhance experimental accuracy and safety. First, galvanized metal sheets were used during coring to prevent particle dispersion, water splashing, and equipment corrosion (Figure 42a). Second, selecting specimens with flat surfaces and rectangular-cuboid shapes optimized coring and minimized material waste (Figure 42b). Third, during dynamic testing, a transparent plexiglass box was placed over the specimens to allow high-resolution video recording of the tests without damaging the camera, effectively capturing the fracture mechanisms (Figure 43).

These measures, combined with careful coring, geometric cutting, creation of non-persistent notches, and environmental conditioning, ensured specimen structural integrity, repeatability, and data reliability. Consequently, this study not only provides insights into the true mechanical behavior of iron ore but also offers a practical guideline for preparing natural rock specimens in the laboratory, enhancing the accuracy and reliability of uniaxial, Brazilian, and dynamic tests.

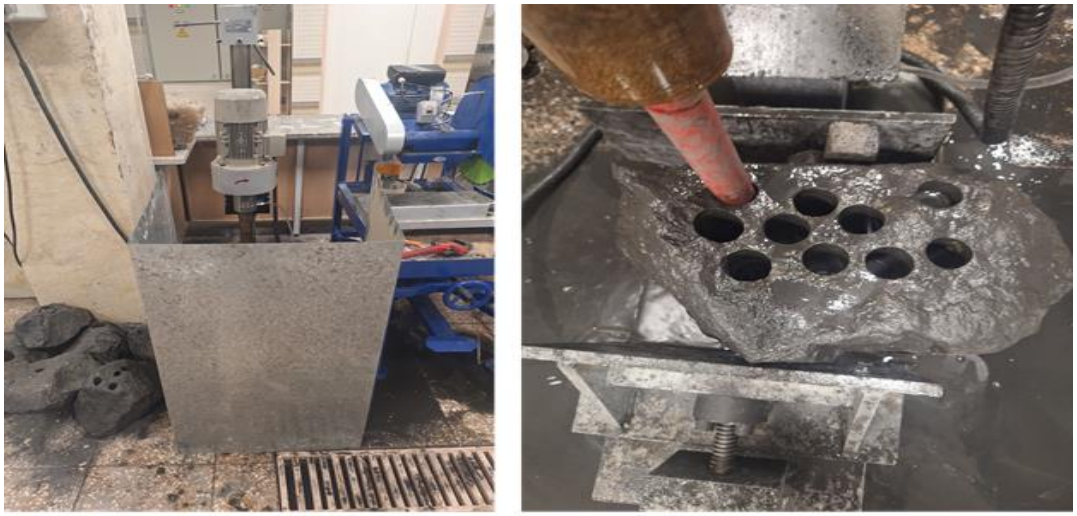

Figure 42. (a) Use of galvanized metal sheets during coring, and (b) coring from specimens with flat surfaces.



Figure 43. Placement of a transparent box over the specimens during SHPB testing.

4. Conclusions

This study comprehensively investigated the preparation methods of iron ore specimens for uniaxial, Brazilian, and dynamic tests. The results demonstrated that meticulous adherence to coring, geometric cutting, end-surface polishing, creation of edge-notched notches with controlled thickness, length, and angle, as well as environmental conditioning of the specimens (dry, saturated, and frozen), plays a critical role in maintaining their structural integrity and quality. Controlling parameters such as drill diameter, alignment of the drill surface, coring speed, and environmental conditions not only ensures measurement accuracy but also enables the simulation of natural fracture patterns and realistic loading conditions. Furthermore, systematic procedures and precise documentation of the geometric and environmental characteristics of specimens enhance the reproducibility and reliability of laboratory.

References

[1]. Hoek, E., & Brown, E. T. (1997). Practical estimates of rock mass strength. *International journal of rock mechanics and mining sciences*, *34*(8), 1165-1186.

[2]. Zhang, X., Jiang, Q., Kulatilake, P. H. S. W., Xiong, F., Yao, C., & Tang, Z. (2019). Influence of asperity morphology on failure characteristics and shear strength properties of rock joints under direct shear tests. *International Journal of Geomechanics*, *19*(2), 04018196.

[3]. Tsiambaos, G., & Saroglou, H. (2010). Excavatability assessment of rock masses using the Geological Strength Index (GSI). *Bulletin of Engineering Geology and the Environment*, *69*(1), 13-27.

[4]. Sarfarazi, V., Asgari, K., Zarei, M., & Ghalam, E. Z. (2022). Behavior of F shape non-persistent joint under experimental and numerical uniaxial compression test. *Advances in concrete construction*, *13*(2), 199-213.

[5]. Fu, J., Sarfarazi, V., Haeri, H., Naderi, K., Fatehi Marji, M., & Guo, M. (2022). The comparison between NBD test results and SCB test results using experimental test and numerical simulation. *Advances in concrete construction*, *13*(1), 83-99.

[6]. Bagher Shemirani, A., Haeri, H., Sarfarazi, V., Ebneabbasi, P., & Fatehi Marji, M. (2023). Investigation of the interaction between concrete-gypsum interface and internal notch using experimental test and numerical simulation. *Mechanics Based Design of Structures and Machines*, *51*(2), 1165-1188.

[7]. Fu, J. W., Haeri, H., Sarfarazi, V., Noshadi, A. H., Marji, M. F., & Guo, M. D. (2022). Investigating the failure behavior of gypsum specimens with non-persistent vertical notch under uniaxial compression. *Strength of Materials*, *54*(1), 14-32.

[8]. Shakeri, J., Asadizadeh, M., & Babanouri, N. (2022). The prediction of dynamic energy behavior of a Brazilian disk containing nonpersistent joints subjected to drop hammer test utilizing heuristic approaches. *Neural Computing and Applications*, *34*(12), 9777-9792.

[9]. Sarfarazi, V., Asgari, K., Maroof, S., & Fattahi, S. (2022). Effects of number and angle of T Shape non persistent cracks on the failure behavior of samples under UCS test. *Computers and Concrete*, *29*(1), 31.

[10]. Fu, J., Haeri, H., Sarfarazi, V., Asgari, K., & Marji, M. F. (2022). The shear behaviors of concrete-gypsum specimens containing double edge cracks under four-point loading conditions. *Theoretical and Applied Fracture Mechanics*, *119*, 103361.

[11]. Fu, J., Sarfarazi, V., Haeri, H., Shahbazian, A., Marji, M. F., & Yu, Y. (2022). Study of tensile crack growth in rock-like materials under punch shear test. *Theoretical and Applied Fracture Mechanics*, *121*, 103509.

[12]. Haeri, H., Sarfarazi, V., & Naderi, A. A. (2022). Shear mechanism of non-persistent notches using punch shear test. *Iranian Journal of Science and Technology, Transactions of Civil Engineering*, *46*(1), 237-250.

[13]. Haeri, H., Sarfarazi, V., Ebneabbasi, P., Shahbazian, A., Marji, M. F., & Mohamadi, A. R. (2020). XFEM and experimental simulation of failure mechanism of non-persistent joints in mortar under compression. *Construction and Building Materials*, *236*, 117500.

[14]. Asadizadeh, M., Karimi, J., Hossaini, M. F., Alipour, A., Nowak, S., & Sherizadeh, T. (2022). The effect of central flaw on the unconfined strength of rock-like specimens: an intelligent approach. *Iranian Journal of Science and Technology, Transactions of Civil Engineering*, *46*(5), 3679-3694.

[15]. Sarfarazi, V. (2020). Study of tensile behavior of Y shape non-persistent joint using experimental test and numerical simulation. *Computers and Concrete, An International Journal*, *26*(6), 565-576.

[16]. Zhou, L., Sarfarazi, V., Haeri, H., Ebneabbasi, P., Fatehi Marji, M., & Hassannezhad Vayani, M. (2023). A new approach for measurement of the fracture toughness using the edge cracked semi-cylinder disk (ECSD) concrete specimens. *Mechanics Based Design of Structures and Machines*, *51*(5), 2896-2917.

[17]. Sarfarazi, V., Abharian, S., & Ghorbani, A. (2021). Physical test and PFC modelling of rock pillar failure containing two neighboring joints and one hole. *Smart Struct. Syst*, *27*(1), 123-137.

[18]. Yang, S. Q., Huang, Y. H., Ranjith, P. G., Jiao, Y. Y., & Ji, J. (2015). Discrete element modeling on the crack evolution behavior of brittle sandstone containing

three fissures under uniaxial compression. *Acta Mechanica Sinica*, *31*(6), 871-889.

[19]. Shaunik, D., & Singh, M. (2019). Strength behaviour of a model rock intersected by non-persistent joint. *Journal of Rock Mechanics and Geotechnical Engineering*, *11*(6), 1243-1255.

[20]. Mohammadi, S. D., Mortezaei, R., Sarfarazi, V., & Salehipor, P. (2025). Delay failure and fast fracturing of notched bedding rock under shear test condition: Physical test and discrete element simulation. *Computational Particle Mechanics*, *12*(1), 673-691.

[21]. Amini, M. S., Sarfarazi, V., & Babanouri, N. (2021). Influence of non-persistent joint sets on the failure behaviour of concrete under uniaxial compression test. *Computers and Concrete*, *28*(3), 289-309.

[22]. Sarfarazi, V., Asgari, K., & Mohamadi Bolban Abad, S. (2022). Interaction between one internal hole and two neighboring joints under uniaxial compression using an experimental test and a numerical simulation. *Journal of Mining and Environment*, *13*(2), 407-420.

[23]. Sarfarazi, V., Abharian, S., & Ghalam, E. Z. (2021). Physical test and PFC2D simulation of the failure mechanism of echelon joint under uniaxial compression. *Computers and Concrete*, *27*(2), 99-109.

[24] Fu, J., Haeri, H., Sarfarazi, V., Abad, S. M. B., Marji, M. F., Saeedi, G., & Yu, Y. (2022). Investigating the effects of non-persistent cracks' parameters on the rock fragmentation mechanism underneath the U shape cutters using experimental tests and numerical simulations with PFC2D. *Structural Engineering and Mechanics, An Int'l Journal*, *83*(4), 495-513.

[25]. Mortezaei, R., Mohammadi, S. D., Sarfarazi, V., & Bahrami, R. (2024). The influence of brittleness of interlayers on the failure behavior of bedding rock; experimental test and particle flow code simulation. *Periodica Polytechnica Civil Engineering*, *68*(1), 169-184.

[26]. Chen, X., Liu, X., Lu, R., & Feng, Z. (2023). Experimental and Numerical Studies on Interaction Mechanism between Joints and a Hole in Rock-like Materials under Uniaxial Compression. *Energies*, *16*(3), 1489.

[27]. Chen, Q., Liu, Y., Wang, W., Ou, X., Zhou, Y., Teng, Z., & Tian, X. (2022). Effects of normal stress and joint inclination angle on rock failure characteristics under compression–shear conditions. *Frontiers in Earth Science*, *10*, 950648.

[28]. Sarfarazi, V., Karimi Javid, H., & Asgari, K. (2021). Study of rock pillar failure consisting of non-persistent joint using experimental test and fracture analysis code in two dimensions. *Journal of Mining and Environment*, *12*(1), 163-179.

[29] Shemirani, A. B., Amini, M. S., Sarfarazi, V., Shahriar, K., Moarefvand, P., & Haeri, H. (2021). Experimental and numerical investigation of the effect of bridge area and its angularities on the failure mechanism of non-persistent crack in concrete-like materials. *Smart Struct. Syst*, *27*(3), 479-492.

[30]. Haeri, H., Sarfarazi, V., Zhu, Z., Hokmabadi, N. N., Moshrefifar, M. R., & Hedayat, A. (2019). Shear behavior of non-persistent joints in concrete and gypsum specimens using combined experimental and numerical approaches. *Struct. Eng. Mech*, *69*(2), 221-230.

[31]. Mortezaie, R., Mohammadi, S. D., & Sarfarazi, V. (2022). Preparation of Heterogeneous Rock-Like Samples Containing Non-Persistent Notch; Different Layout. *Journal of Mining and Environment*, *13*(4), 1139-1157.

[32]. Pan, W., Liang, S., Gao, P., Zhao, Z., & Deng, Y. (2024). Study on Mechanical Properties of Fractured Sandy Mudstone Based on Triaxial Compression Experiment. *Applied Sciences*, *14*(16), 7204.

[33]. Mohammadi, S. D., Mortezaei, R., Sarfarazi, V., & Far, A. M. (2025). Crack growth properties and AE phenomena in notched hard/soft layered rock under punch shear test; experimental test and numerical simulation. *Results in Engineering*, 106652.

[34]. Wang, Q., Chen, W., Peng, W., Wang, Y., Zhou, Y., & Peng, Z. (2025). Uniaxial compressive damage evolution and constitutive modeling of fissure-like rocks under different loading rates based on acoustic emission. *Scientific Reports*, *15*(1), 2119.

[35]. Sarfarazi, V., Haeri, H., Bagheri, F., Zarrin Ghalam, E., & Fatehi Marji, M. (2022). PFC simulation of Brazilian tensile strength test in geomaterials' specimens with T-shaped non-persistent joints. *Journal of Mining and Environment*, *13*(4), 1189-1209.

[36]. Rezaei, A., Sarfarazi, V., Babanouri, N., Omidi Manesh, M., & Jahanmiri, S. (2023). Failure Mechanism of Rock Pillar Containing Two Edge Notches: Experimental Test and Numerical Simulation. *Journal of Mining and Environment*, *14*(3), 961-971.

[37]. Sarfarazi, V., Haeri, H., Fatehi Marji, M., Saeedi, G., & Namdarmanesh, A. (2023). Investigation of Shear Properties of Open Non-persistent Latitudinal Discontinuities of Same Level. *Journal of Mining and Environment*, *14*(4), 1361-1371.

[38]. Li, X., Zhou, T., & Li, D. (2017). Dynamic strength and fracturing behavior of single-flawed prismatic marble specimens under impact loading with a split-Hopkinson pressure bar. *Rock Mechanics and Rock Engineering*, *50*(1), 29-44.

[39]. Yan, Z., Dai, F., Liu, Y., & Du, H. (2020). Experimental investigations of the dynamic mechanical properties and fracturing behavior of cracked rocks under dynamic loading. *Bulletin of Engineering Geology and the Environment*, *79*(10), 5535-5552.

[40]. Yan, Z., Dai, F., Zhu, J., & Xu, Y. (2021). Dynamic cracking behaviors and energy evolution of multi-flawed rocks under static pre-compression. *Rock Mechanics and Rock Engineering*, *54*(9), 5117-5139.

[41]. Zhao, G., Zhang, L., Dai, B., Liu, Y., Zhang, Z., & Luo, X. (2022). Experimental Investigation of Pre-Flawed Rocks under Dynamic Loading: Insights from Fracturing Characteristics and Energy Evolution. *Materials*, *15*(24), 8920.

[42]. Wang, Q., Shi, F., Wang, X., Meng, Q., Li, X., Song, J., & Yu, C. Y. (2022). Dynamic mechanical response, cracking behavior, and stress intensity factors of cement mortar specimens with open and closed flaws. *Shock and Vibration*, *2022*(1), 5956525.

[43]. Kumar, S., Tiwari, G., Parameswaran, V., & Das, A. (2022). Rate-dependent mechanical behavior of jointed rock with an impersistent joint under different infill conditions. *Journal of Rock Mechanics and Geotechnical Engineering*, *14*(5), 1380-1393.

[44]. Lei, W., Wenjie, F., Mingye, L., & Junhong, Y. (2023). Crack Propagation and Fragmentation Characteristics of Single-Flawed Sandstone Samples under Different Loading Conditions. *Shock and Vibration*, *2023*(1), 2621704.

[45]. Ji, D., Cheng, H., & Zhao, H. (2024). Damage effect and progressive failure mechanism of sandstone considering different flaw angles under dynamic loading. *Rock Mechanics Bulletin*, *3*(1), 100085.

[46]. Zhou, H. Y., Liu, D. S., Gao, Z. H., Chi, E. A., Rao, J. Y., & Hu, T. (2024). Dynamic failure characteristics of sandstone containing different angles of pre-existing crack defects. *Mathematics*, *12*(11), 1651.

[47]. Ping, Q., Sun, S., Li, X., Wu, S., Xu, Y., Hu, J., & Hu, W. (2024). Analysis of the Dynamic Mechanical Properties and Energy Dissipation of Water-Saturated Fissured Sandstone Specimens. *Applied Sciences*, *14*(4), 1368.

[48]. Yin, T., Lu, J., Guo, W., Wu, Y., & Ma, J. (2024). Dynamic mechanical response and damage constitutive model of end-jointed rock bridge with different water content states under impact load. *Theoretical and Applied Fracture Mechanics*, *130*, 104255.

[49]. Zou, C., Wong, L. N. Y., & Cheng, Y. (2012, June). The strength and crack behavior of the rock-like gypsum under high strain rate. In *ARMA US Rock Mechanics/Geomechanics Symposium* (pp. ARMA-2012). ARMA.

[50]. Yaylaci, M., Yaylı, M., Öztürk, Ş., Ay, S., Özdemir, M. E., Yaylaci, E. U., & Birinci, A. (2024). Examining the contact problem of a functionally graded layer supported by an elastic half-plane with the analytical and numerical methods. *Mathematical Methods in the Applied Sciences*, *47*(12), 10400-10420.

[51]. Öner, E., Yaylaci, E. U., & Yaylacı, M. (2024). Multi-method examination of contact mechanics in orthotropic layers under gravity. *Mechanics of Materials*, *195*, 105036.

[52]. Yaylaci, M., Öner, E., Adıyaman, G., Öztürk, Ş., Uzun Yaylacı, E., & Birinci, A. (2024). Analyzing of continuous and discontinuous contact problems of a functionally graded layer: theory of elasticity and finite element method. *Mechanics Based Design of Structures and Machines*, *52*(8), 5720-5738.

[53]. Yaylaci, M., Yazıcıoğlu, A., Yaylacı, E. U., Terzi, M., & Birinci, A. (2025). Evaluation of the contact problem of two layers one of functionally graded, loaded by circular rigid block and resting on a Pasternak foundation by analytical and numerical (FEM and MLP) methods. *Archive of Applied Mechanics*, *95*(4), 1-23.

[54]. Öner, E., Oktay, M. G., Uzun Yaylaci, E., Yaylaci, M., & Mirzaloğlu, İ. (2025). Tri-method analysis of contact mechanics in orthotropic-isotropic materials. *Archive of Applied Mechanics*, *95*(5), 116.

[55]. Yazıcıoğlu, A., Yaylaci, M., Sekban, D. M., Kuleyin, H., Yaylacı, E. U., Birinci, A., & Mahmoud, S. R. (2025). Analysis of the contact problem functionally graded layer placed on a Pasternak foundation. *ZAMM-Journal of Applied Mathematics and Mechanics/Zeitschrift für Angewandte Mathematik und Mechanik*, *105*(8), e70152.

[56]. Aktarer, S. M., Kucukomeroglu, T., Sekban, D. M., Yaylaci, E. U., Yaylaci, M., Ozdemir, M. E., & Mirzaloglu, I. (2025). Analysis of the changes in microstructure, mechanical, and contact properties of multi-pass friction stir processed DP800 steel. *Advances in nano research*, 253-264.

[57]. Sekban, D. M., Yaylaci, E. U., Özdemir, M. E., Yaylacı, M., & Tounsi, A. (2025). Investigating formability behavior of friction stir-welded high-strength shipbuilding steel using experimental, finite element, and artificial neural network methods. *Journal of Materials Engineering and Performance*, *34*(6), 4942-4950.

انجمن مهندسی معدن ایران
نشریه مهندسی معدن و محیط زیست
نشانی نشریه: www.jme.shahroodut.ac.ir
دانشگاه صنعتی شاهرود

آماده‌سازی نمونه‌های سنگ‌آهن دارای شکاف نامتد لبه‌ای برای انجام آزمون‌های دینامیکی: هندسه و پیکربندی شکاف‌ها

شادمان محمدی بلبان‌آباد[۱]، وهاب سرفرازی[۲*] و مسعود منجزی[۱]

۱. گروه مهندسی معدن، دانشکده معدن و مواد، دانشگاه تربیت‌مدرس، تهران، ایران
۲. گروه مهندسی معدن، دانشگاه صنعتی همدان، همدان، ایران

اطلاعات مقاله

تاریخ ارسال: ۲۰۲۵/۰۹/۰۴
تاریخ داوری: ۲۰۲۵/۱۱/۲۱
تاریخ پذیرش: ۲۰۲۵/۱۱/۲۹

DOI: 10.22044/jme.2025.16775.3292

کلمات کلیدی

دستگاه تست فشاری هاپکینسون
شکاف نامتد لبه‌ای
آزمون دینامیکی
روش آماده‌سازی نمونه

چکیده

یکی از مراحل حیاتی در پژوهش‌های آزمایشگاهی، آماده‌سازی دقیق نمونه‌ها است. این مطالعه با هدف توسعه و ارائه یک روش‌شناسی جامع برای آماده‌سازی نمونه‌های سنگ‌آهن مگنتیتی دارای شکاف‌های نامتد لبه‌ای جهت آزمون‌های دینامیکی، و همچنین نمونه‌های سنگ‌آهن و یخ برای آزمون‌های تک‌محوره و برزیلی انجام شده است. مغزه‌گیری با استفاده از سرمته‌های الماسه با قطر ۵۴ میلی‌متر برای آزمون‌های تک‌محوره و برزیلی و قطر ۲۲ میلی‌متر برای آزمون‌های دینامیکی بارگذاری ضربه‌ای هاپکینسون (SHPB) انجام شد. شکاف‌های نامتد لبه‌ای با ضخامت ۳ میلی‌متر و با طول و شیب کنترل‌شده توسط دستگاه برش ایجاد شدند و کیفیت هندسی آن‌ها از طریق اندازه‌گیری دقیق مورد تأیید قرار گرفت. برای نمونه‌های یخ، پر کردن شکاف‌ها با آب در لوله‌هایی هم‌قطر با نمونه، یکنواختی و پایداری بهینه را ایجاد کرد. علاوه بر این، کنترل دقیق پارامترهایی نظیر موازی بودن مغزه و مته، سرعت حفاری، جریان آب خنک‌کننده، و شرایط محیطی (خشک، اشباع و یخ‌زده) موجب حفظ یکپارچگی ساختاری و کیفیت نمونه‌ها شد. نتایج نشان داد که ترتیب دقیق انجام این مراحل، همراه با مستندسازی دقیق ویژگی‌های هندسی و محیطی نمونه‌ها، امکان تولید نمونه‌هایی سالم، استاندارد و قابل تکرار را فراهم کرده و بررسی قابل اعتماد و سازگار رفتار مکانیکی و شکست سنگ‌آهن مگنتیتی را تحت شرایط بارگذاری دینامیکی و شبه‌استاتیکی تضمین می‌کند.

نویسنده مسئول مکاتبات: Sarfarazi@hut.ac.ir (و. سرفرازی)